THE
ASTROPHYSICAL JOURNAL
AN INTERNATIONAL REVIEW OF SPECTROSCOPY
AND ASTRONOMICAL PHYSICS

VOLUME XXXIII MAY 1911 NUMBER 4

THE POSITION OF CERTAIN CORONAL STREAMS ON THE ASSUMPTION THAT THE CORONA IS A MECHANICAL PRODUCT

By JOHN A. MILLER

INTRODUCTION

The present investigation had its genesis in an attempt to apply Schaeberle's mechanical theory of the sun's corona[1] to the streams of the corona of 1905. I decided, after some investigation, to modify, in some respects radically, the assumptions made by Professor Schaeberle and to consider the streamers of the corona as the projection on a plane of streams of particles, the motion of which is produced by ejection, by the rotation of the sun, by the attraction of the sun, and by the radiant pressure of the sun.

The theoretical results made it desirable to examine a great number of large-scale photographs of the corona. Director Campbell generously placed at my disposal the most excellent series at the Lick Observatory. The present paper is a discussion of streamers found on these plates. Briefly stated, the results of the investigation indicate a mechanical origin of the corona, at least thus far:

If the streamers of the corona are formed of particles acted on by the forces named above and under the assumptions stated more explicitly later, streams of a certain shape must theoretically

[1] J. M. Schaeberle, *A Mechanical Theory of the Solar Corona*, p. 47; total solar eclipse of December 1889, etc., Lick Observatory.

result. Streams of this shape are found on the plates, and, under the same assumptions, it has been possible to find their heliocentric positions and the magnitude of the radiant pressure acting on particles in them.

I am under many obligations. Director Campbell not only put at my disposal all the coronal photographs of the Lick Observatory, but aided me in many ways when I was measuring them. Professor Marriott of Swarthmore College aided me, not only in making the computations, but discussed with me the entire theory and suggested improvements in the methods of solution. Mr. C. J. Olivier very effectively aided me in the computations, as did my own students, Mr. J. H. Pitman, Miss H. W. Sheppard, Mr. G. C. Carr, and Mr. J. A. White, Mr. Pitman sharing in the computation of six streamers.

THE THEORY

If it is assumed that the sun's corona is caused by light emitted and reflected by particles ejected from the sun by forces which in general act along lines normal to the sun's surface and that these particles follow each other closely enough to make a continuous stream, it follows from the laws of mechanics that of two particles of the same stream that one has the smaller angular velocity which is farther from the sun. Moreover, if any particle, after leaving the sun's surface, is acted upon by forces the resultant of which passes through the center of the sun, it will move in a plane passing through the sun's center, tangent to the small circle on the sun's surface described by the point of ejection. The plane of the subsequent orbit of the particle will therefore be perpendicular to a meridian of the sun passing through the point of ejection. In Fig. 1, P_1 is the pole of the sun; C its center; the xy-plane, the plane of the sun's equator; P_0 is the point of ejection; CX is the radius of the sun passing through its west side. The particle ejected from the point P_0 will move in a plane passing through P_0C and perpendicular to the arc P_1P_0.

These assumptions require that the sun be a sphere and that the resultant of all forces of radiant pressure acting on a particle is normal to the sun's surface.

If we assume, further, that the resultant of all forces that act

on a particle after it leaves the sun's surface varies inversely as the square of the distance of the particle from the center of the sun, it (the particle) will describe a conic section with the center of the sun as one focus. That is, under these assumptions a stream of the corona is made up of particles each moving in a conic section but no two of which are moving in the same plane. In fact, the

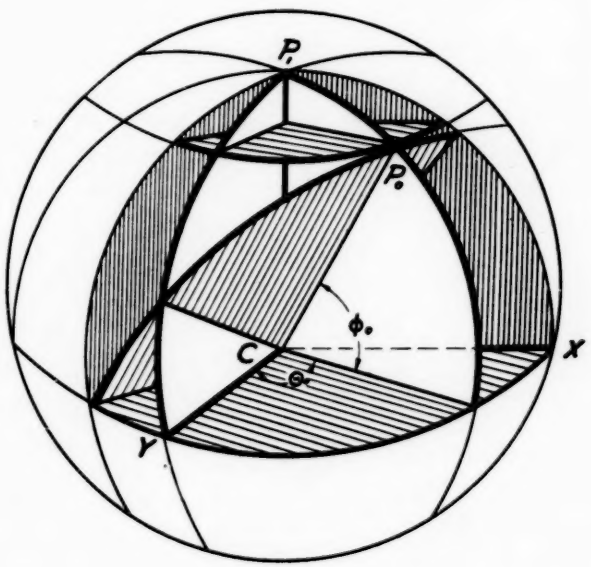

FIG. 1

planes of the orbits of the various particles will be tangent to a circular cone, the vertex of which is at the center of the sun and the base of which is a small circle described by the point of ejection. The stream itself is, of course, not a plane curve.

If what we see and photograph as a *streamer*[1] of the sun's corona is one of those *streams* of particles projected orthogonally on a plane perpendicular to the line joining the observer's eye to the center of the sun, it is possible to prove that some of these streamers

[1] Throughout this paper I shall mean by a *stream* the actual stream of the particles in the corona. By a *streamer* I shall mean the orthographic projection of a stream. By the *base* of a stream, I shall mean the intersection of the stream and the margin of the moon's shadow.

will curve throughout their entire length away from the projection of the pole of the sun, others will curve toward it, while a few others will curve first toward it and afterward away from it, or vice versa. That is, from the center of the sun, C, draw radii vectores to the successive points a, b, c in the streamer (Figs. 2, 3, 4). Choose as the initial line CW, W being the west side of the sun; then the vectorial angle WCa always decreases as the extremity of the radius vector describes the streamer, as in Fig. 2. Or it always increases as in Fig. 3; or it increases first and then decreases, or vice versa as in Fig. 4. It is hardly necessary to say that in these drawings the amount of curvature is exaggerated. I shall consider here the class of streamers last described — those shown in Fig. 4. For this class of streamers it is possible to find the heliocentric latitude and longitude of a particle at that point of the streamer at which the radius vector is tangent; as, for example, the point P in Fig. 4. We can find the distance of this particle from the

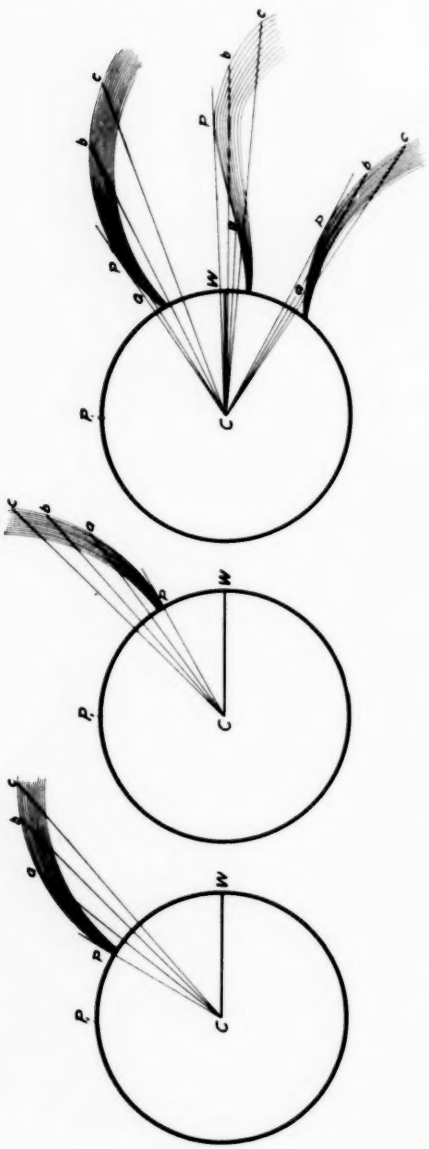

FIG. 4

FIG. 3

FIG. 2

sun, the point on the sun's surface from which the particle was ejected, the time it was ejected, and hence the position of the point of ejection at any time; we can also find the velocity with which the particle was ejected, the velocity of the particle at any time, the orbit of each particle in the stream, and the resultant of all forces acting on the particle, and, if we assume the law of the force, we can find the magnitude of any repulsive force, such as light or electric pressure, that may exist.

If we pass a plane through the line joining the center of the sun and the observer and through the west side of the sun; and another plane through the same line and a point on the *stream;* the vectorial angle to the corresponding point on the *streamer* measures the angle between these planes. This angle can be measured in the photograph.

We shall now make a mathematical statement of the problem.

Choose as

z-axis, the axis of the sun;

x-axis, the equatorial diameter passing through the west side of the sun;

y-axis, a line perpendicular to the xz-plane.

Let x, y, z be the rectangular heliocentric co-ordinates of any point;

Let ϕ_1 be its heliocentric latitude;

Let θ_1 be its heliocentric longitude, measured from the yz-plane, positive in the direction of the sun's rotation;

Let R_1 be its radius vector;

Let A_1 be the vectorial angle of the point on the streamer corresponding to this point;

Let λ be the angle between the z-axis and the line through the observer and the center of the sun;

Let the x- and the z-axis project into a ξ- and η-axis respectively;

Let A be the angle that the projection of a radial line makes with the ξ-axis.

Then,

$$\left.\begin{aligned} x &= R_1 \cos \phi_1 \sin \theta_1, \\ y &= R_1 \cos \phi_1 \cos \theta_1, \\ z &= R_1 \sin \phi_1 \end{aligned}\right\}$$

$$\xi = x,$$

$$\eta = z \sin \lambda - y \cos \lambda,$$

$$\tan A_1 = \frac{\sin \lambda \tan \phi_1 - \cos \lambda \cos \theta_1}{\sin \theta_1} \qquad (a)$$

We know that as we pass successively from one point of the streamer to another, starting at the base, θ_1 constantly decreases. Therefore if

$$\frac{d}{d\theta_1}(\tan A_1) \gtrless 0$$

for one point on the streamer, it is for every point unless for some point on the stream the quantities θ_1 and ϕ_1 satisfy the equation

$$\frac{d}{d\theta_1}(\tan A_1) = 0 \qquad (b)$$

Differentiating (a) with regard to θ_1 we see that, since

$$\frac{d\phi_1}{d\theta_1} \neq \infty$$

$\frac{d}{d\theta_1}(\tan A_1)$ can be infinity if, and only if, $\phi_1 = \pm 90°$; or if $\theta_1 = 0°$ or $180°$. That is, the stream is either at the pole of the sun or directly behind or in front of the sun. In either case the vectorial angle is $90°$; and, except in rare cases, the stream would be invisible. We shall therefore leave this case out of consideration. Hence the streamer curves in one direction only, unless an equation (b) exists. Since (a) contains only two unknowns one would surmise that (b), if it exists, would be the additional equation necessary to solve for these quantities. This is indeed true, a statement I now propose to prove.

Let P be that point in the *stream* that is projected into that point on the *streamer* at which the radius vector (in the photograph) is tangent to the *streamer*.

Let P_0 be the point on the sun from which P was ejected;

Let P' be a particle at any point in the streamer;

Let P'_0 be the point of ejection of P';

Let t be the time at which the photograph was made;

Let t_0 and t'_0 be the time when P and P' left the sun respectively;

Let θ, ϕ, R, w = respectively, the heliocentric longitude, heliocentric latitude, radius vector, and true anomaly of P at the time t;

Let θ_0, ϕ_0, R_0, w_0 = respectively like values for P_0 at time t_0;

Let θ', ϕ', R', w' = respectively like values for P' at time t;

Let θ'_0, ϕ'_0, R'_0, w'_0 = respectively like values for P'_0 at time t'_0;

Let P and P' project respectively into π and π';

Let ρ and ρ' be the radius vector of π and π' respectively;
Let A and A' be the vectorial angles of π and π' respectively;
Let v_2 = velocity of ejection;
Let v_1 = velocity of the particle due to the sun's rotation;
Let V = velocity with which the particle left the sun;
Let e = eccentricity of the orbits;
Let a = semi-major axis of the orbits;
Let ω = angular velocity of the sun;
Let n = the mean motion in the orbit;
Let C^2 = the constant entering into the differential equations of motion;
Let ψ = angle between the normal to the sun and the initial velocity.

In the computations we have chosen as P' the point which projects into the base of the streamer. If we assume that P and P' have been acted on by the same forces, the particles are describing equal orbits. Hence a, e, and w_0 are the same for every particle of a given stream.

Let P_1 be the pole of the sun.

Project radially from the center of the sun the points P_1, P_0, P'_0, P, and P' into the points p_1, p_0, p'_0, p, and p' respectively on the surface of a sphere concentric with the sun. Then

$$\begin{aligned}
&\text{arc } p_1p_0 = 90^\circ - \phi_0,\\
&\text{arc } p_1p \;= 90^\circ - \phi,\\
&\text{arc } p_1p' = 90^\circ - \phi',\\
&\text{arc } p_0p \;= w - w_0,\\
&\text{arc } p'_0p' = w' - w_0.
\end{aligned}$$

We obtain from the spherical triangle p_0p_1p the following relations:

$$\sin (w-w_0) = \sin (\theta-\theta_0) \cos \phi \cdot \qquad (c)$$
$$\tan (w-w_0) = \tan (\theta-\theta_0) \cos \phi_0 \qquad (1)$$
$$\tan \phi = \cos (\theta-\theta_0) \tan \phi_0 \qquad (2)$$
$$\sin \phi = \cos (w-w_0) \sin \phi_0 \qquad (3)$$

There are four similar relations for the triangle p'_0p_1p'.

Projecting R and ρ on the x-axis we get

$$\rho \cos A = R \cos \phi \sin \theta \qquad (4)$$

Similarly,

$$\rho' \cos A' = R' \cos \phi' \sin \theta' \qquad (5)$$

Now θ and ϕ satisfy the equation

$$\tan A = \frac{\sin \lambda \tan \phi - \cos \lambda \cos \theta}{\sin \theta} = \frac{\sin \lambda \cos (\theta - \theta_\circ) \tan \phi_\circ - \cos \lambda \cos \theta}{\sin \theta} \qquad (6)$$

The co-ordinates of a second point on the stream nearer than P to the sun satisfy the equation

$$\tan A + \Delta \tan A = \frac{\sin \lambda \cos (\theta + \Delta\theta - \theta_\circ - \Delta\theta_\circ) \tan \phi_\circ - \cos (\theta + \Delta\theta) \cos \lambda}{\sin (\theta + \Delta\theta)}.$$

Subtracting these two equations, dividing by $\Delta\theta$, taking the limit and putting

$$\frac{d}{d\theta}(\tan A) = 0,$$

we obtain

$$\frac{d\theta_\circ}{d\theta} = \frac{\cos \theta_\circ - \cot \lambda \cot \phi_\circ}{\sin \theta \sin (\theta - \theta_\circ)} \qquad (d)$$

Also the co-ordinates of P and the second point on the streamer nearer the sun satisfy respectively the equations

$$\tan (\theta - \theta_\circ) \cos \phi_\circ = \tan (w - w_\circ),$$

and

$$\tan (\theta + \Delta\theta - \theta_\circ - \Delta\theta_\circ) \cos \phi_\circ = \tan (w - \Delta w - w_\circ).$$

Treating these equations in the same way we obtain

$$1 - \frac{d\theta_\circ}{d\theta} = \frac{-\sec^2 (w - w_\circ) \frac{dw}{d\theta}}{\cos \phi_\circ \sec^2 (\theta - \theta_\circ)} = \frac{\sec^2 (w - w_\circ)}{\sec^2 (\theta - \theta_\circ) \cos \phi_\circ} \quad \frac{\frac{dw}{dt} \cdot \frac{d\theta_\circ}{d\theta}}{\omega}.$$

Now w is the true anomaly of a particle that has moved in its orbit for a time $(t - t_\circ)$, and its radius vector has described the angle $(w - w_\circ)$. If the particle had moved for the time $t - \Delta t - t_\circ$, it would have moved through an angle $w - \Delta w - w_\circ$. Now the second particle left the sun at a time $t_\circ + \Delta t$. It has therefore moved in its orbit for a time $t - \Delta t - t_\circ$. Its true anomaly is therefore $w - \Delta w - w_\circ$. That is, the difference of the true anomaly of the two successive particles in a stream is the same as the difference of the true anomaly of two positions of a particle in its orbit at the time t and $t - \Delta t$. That is, as we trace a streamer, tracing toward the sun, the true

anomaly of the successive particles that we encounter changes at the same rate as the true anomaly of a particle moving in its orbit. Hence we may write

$$\frac{dw}{dt}=\frac{C^2\sqrt{a(1-e^2)}}{R^2}.$$

This is merely the numerical value of $\frac{dw}{dt}$, the sign being given to Δw.

Now,

$$n^2a^3=C^2$$

$$\tan\psi=\frac{v_1}{v_2}$$

$$4a^2e^2=R_\circ^2+(2a-R_\circ)^2+2R_\circ(2a-R_\circ)\cos 2\psi$$

$$v_1=\omega R_\circ\cos\phi_\circ$$

$$v_1^2+v_2^2=V^2$$

$$V^2=C^2\left[\frac{2}{R_\circ}-\frac{1}{a}\right]$$

We shall now put $R_\circ=1$.

Substituting from the above equations we obtain,

$$\frac{dw}{dt}=\frac{\cos\phi_\circ\,\omega}{R^2}$$

Reducing we obtain

$$\frac{d\theta_\circ}{d\theta}=\frac{\rho^2\cos^2 A}{\rho^2\cos^2 A-\sin^2\phi_\circ\cot^2\phi\sin^2\theta\cos^2(\theta-\theta_\circ)} \qquad (e)$$

Equating (d) and (e) and eliminating by the preceding equations, remembering the identity,

$$\cos\theta_\circ=\cos(\theta-\theta_\circ)\cos\theta+\sin(\theta-\theta_\circ)\sin\theta$$

we obtain

$$+\tan^2(\theta-\theta_\circ)\left[-P_1\tan^3\theta+g\tan^2\theta+k\tan\theta+\frac{P_3}{2}\right]$$
$$+\tan(\theta-\theta_\circ)[-P_7\tan^3\theta-P_8\tan^2\theta]+[-f\tan^3\theta$$
$$+h\tan^2\theta+j\tan\theta+m]=0 \qquad (7)$$

where

$$f=P_1+P_{10}-P_8, \qquad j=2P_1-P_5-P_{10},$$
$$g=P_2-P_3, \qquad k=2P_1-P_5,$$
$$h=P_2+P_{13}-P_3-P_7, \qquad m=\frac{P_3}{2}+P_{13},$$

and where

$$P_1=\rho^2a^2b^2d, \qquad P_7=bc^2, \qquad a=\cos A,$$
$$P_2=\rho^2a^2b^3, \qquad P_8=c^2d, \qquad b=\tan A,$$
$$P_3=2\rho^2a^2bd^2, \qquad P_{10}=\rho^2a^2c^2d, \qquad c=\sin\lambda,$$
$$P_5=\rho^2a^2d^3, \qquad P_{13}=\rho^2a^2bc^2, \qquad d=\cos\lambda.$$

We have also

$$R=\frac{a(1-e^2)}{1+e\cos w} \tag{8}$$

$$R'=\frac{a(1-e^2)}{1+e\cos w'} \tag{9}$$

$$1=\frac{a(1-e^2)}{1+e\cos w_\circ} \tag{10}$$

$$\tan A'=\frac{\sin\lambda\tan\phi'-\cos\lambda\cos\theta'}{\sin\theta'} \tag{11}$$

$$n(t'_\circ-t_\circ)=\int_{R'}^{R}\frac{RdR}{a\sqrt{a^2e^2-(a-R)^2}} \tag{12}$$

$$\theta'_\circ-\theta_\circ=\omega(t'_\circ-t_\circ) \tag{13}$$

Now a large change in θ produces a small change in ϕ when $\theta-\theta_\circ$ is small; except in very high latitudes. Hence if we choose for P' the point in the streamer at the edge of the moon's shadow, we can without sensible error put $\phi'=\phi_\circ$.

The solution requires one other equation involving a linear quantity. I have chosen as this quantity the aphelion distance, $a(1+e)$. If we measure the greatest extension of the streamer, we know that $a(1+e)$ cannot be less than this measured distance. Its maximum value is much less definite. The stream may not have reached its greatest height, or the entire stream may not have been photographed. In the computations of the streamers discussed later there are certain limits beyond which, in a given case, $a(1+e)$cannot go; and actual computations show that one can change $a(1+e)$ within rather large limits without effecting large changes in either θ or ϕ. However, a change in $a(1+e)$ does change $t-t_\circ$ and hence changes the position of the point of ejection at any time. This measured quantity, $a(1+e)$, completes the number of equations required to solve our problem.

Since, however, some of the equations are transcendental, it is not easy to solve them. Analytically, we should, in general, expect that more than one set of values would satisfy them; but in addition to these equations, the values admissible to our problem must satisfy the inequalities,

$$\left.\begin{array}{l} \theta < \theta' \\ |\phi'| < |\phi_0| \\ |\phi| < |\phi'| \end{array}\right\} \text{if } (\theta - \theta_0) < 90^\circ$$
$$R' < R$$
$$\tan^2 \phi' < \frac{\cos^2 \lambda + \tan^2 A}{\sin^2 \lambda} \qquad (14)$$

The method that we adopted in the solution of these equations is as follows: We substituted in (7) a value of tan θ arbitrarily chosen and solved for tan $(\theta - \theta_0)$. To guide us in our choice of tan θ we formed the discriminant of equation (7), regarding tan θ as a part of the coefficients. Since no value of tan θ that made this discriminant negative was admissible, the range of our choice was thereby limited. Having found a value of tan θ that gave real values of tan $(\theta - \theta_0)$, we solved the equations *seriatim*, having care that none of the values thus found violates the inequalities (14). By virtue of this arbitrary choice of tan θ we have one more equation than is necessary for solution. Accordingly in our trial solution we did not make use of equation (13). The true solution must, however, satisfy this equation and therefore we used it as a check. That is, the test of the solution is that the *angular velocity of the sun multiplied by the difference between the time of ejection of two particles must equal the difference of the longitudes of the points of ejection of these particles*. If this check was not satisfied we rejected the solution and tried another value for tan θ.

This theory is, in some respects, the same as that given by the writer in the *Astrophysical Journal*, **27**, 286–295, 1908. However, equations (4) and (5) of that article are not true. They have been replaced by (7) of the present paper. I have also improved the method of the solution of these equations. For these reasons I have presented it here giving the details of the solutions.

APPLICATION OF THIS THEORY TO THE LICK PHOTOGRAPHS

This theory had been applied, with gratifying results, to the large-scale photographs made by Professor Cogshall and myself in 1905.[1] At the invitation of Director Campbell, I spent a part of the summer of 1909 at Lick Observatory measuring the very complete set of large-scale photographs made, since 1893, by eclipse parties of that observatory. This afforded a severe test of this theory, because (1) too much cannot be said commending the uniform excellence of these plates; (2) the series is very complete: it contains photographs of every total solar eclipse, except one, when it was cloudy, that has occurred since 1893, viz., those of 1893, 1898, 1900, 1901, 1905, and 1908; (3) the period covers more than one sun-spot cycle; (4) the different eclipses occurred when the axis of the sun was inclined at various angles to the line of sight, the inclination being approximately 82° in 1905; 95° in 1893; 91° in 1900, and for the other dates somewhere within those limits; (5) all the large-scale photographs were compared with others made with lenses of shorter focus. The plates made in 1905 by Professor Campbell's party in Spain were checked by those made by Professor Hussey in Egypt with an instrument that was a duplicate of the one used in Spain. They were also checked by the plates made by Professor Cogshall and myself also in Spain but with an instrument of different type—the Lick photographs all being made by the familiar ingenious method devised by Schaeberle. Our photographs were made with a horizontal telescope fed by a coelostat. The plates of 1900 were checked by those made by the Smithsonian Institution, loaned to me by the director.

The measures of the plates were necessarily approximate compared with measures of precision. I measured the original negatives on the glass side. The film of the negative rested on a ground glass behind which were electric lights whose intensity and position the operator could change at will. The angles were measured with a protractor reading (by vernier) to minutes. All the streamers except three were measured on three different days, and on each day each measure was repeated from three to seven times.

[1] *Astrophysical Journal*, **27**, 286, 1908.

The equator and the center of the sun were determined by the orientation of the plate at the time of the exposure, and were determined once only.

From the entire series I selected 22 streamers that seemed to have the shape required. I afterward rejected six of these either because I was uncertain whether or not the streamers really reversed their direction of curvature, or because it was impossible to tell where their bases came to the margin of the moon's shadow. Most of these were verified either by Director Campbell, Dr. Albrecht, or Mr. Olivier. There are other streamers that might have been added to this list, but I regarded them as being too uncertain in one or more of the essential particulars. The sixteen streamers chosen are, in my judgment, all that should be included, and there is no doubt that all of these are of the type described in Fig. 4.

Below is a résumé of the measures. A and A' were measured from the western extremity of the sun's diameter, positive in a counter-clockwise direction, and ρ and ρ' were measured in terms of the radius of the sun.

TABLE I

Streamer	A	A'	λ	Log ρ	Greatest Extension of Streamer in Inches
I 1893....	193° 30′	197° 29′	95 21′ 29″	.18002	7.5
II 1893....	197 34	196 06	95 21 29	.31054	7.5
I 1898....	− 4 43	− 7 46	95 21 12	.17142	5.5
II 1898....	17 15	18 48	95 21 12	.29315	6.5
I 1900....	−23 30	−22 14	90 58 02	.04135	5.3
II 1900....	−27 32	−24 59	90 58 02	.04659	5.3
I 1901....	188 35	173 45	92 13 17	.25230	5.0
II 1905....	105 30	103 34	82 49 56	.10480	4.2
III 1905....	263 53	267 58	82 49 56	.10032	3.7
V 1905....	−20 21	−24 10	82 49 56	.24494	6.7
VI 1905....	−30 54	−36 48	82 49 56	.18842	6.7
I 1908....	253 00	251 55	93 21 48	.14768	5.0
II 1908....	244 25	232 31	93 21 48	.18638	8.5
III 1908....	241 11	227 45	93 21 48	.21249	8.5
IV 1908....	198 42	200 55	93 21 48	.18146	4.9
VI 1908....	190 26	191 35	93 21 48	.15335	5.5

Below I append some notes made while measuring these streamers.

1893

This eclipse lasted 186 seconds. Eight plates were exposed. I measured No. 4, which was exposed for eight seconds, beginning 50 seconds after totality began. Plate No. 5 and the plates made with the Dallmeyer lense were used as checks. The streamers on these plates were the most perplexing of the series. The corona around the entire edge of the moon was complex, being made up of a great number of interlacing streamers. It was oftentimes difficult, sometimes impossible, to decide certainly which of two streamers from their point of intersection proceeded in a given direction. Two streamers seemed to me to meet the conditions. They leave the moon's margin at nearly the same place and intersect each other twice. Both are sharp on the convex side of the streamer. Director Campbell expressed some doubt as to the existence of streamer No. II. It was my judgment, however, that it was more certain than streamer No. I. A reference to Table II shows that No. II could not be solved.

1898

This eclipse lasted 159 seconds. Twelve plates were exposed. I measured No. 5, exposed for eight seconds, beginning 43 seconds after totality began. The checks were made with No. 6, and the Floyd plates. Both streamers, No. I and No. II, are well defined. They are sharp on the convex side. The bases are well defined.

1900

This eclipse lasted 90 seconds. Ten plates were exposed. I measured No. 5, exposed for 16 seconds, beginning 42 seconds after totality began. The checks were with No. 2, the Floyd plates, and a plate made by the Smithsonian Institution with the 135-foot telescope. Streamers No. I and No. II are between two prominences, are definite, but are not smooth, being somewhat crinkly. They curve first toward the greater prominence, then away from it.

1901

This eclipse lasted 6 minutes, 9 seconds. Twelve plates were exposed. I measured No. 7, exposed for 150 seconds. This

streamer is well defined and very sharp on the convex side. It apparently originated about 12° south of the southern extremity of a large disturbed region.

1905

This eclipse lasted 3 minutes, 45 seconds. Ten plates were exposed. I measured No. 4, exposed for 8 seconds, beginning 24 seconds after totality began. Streamer No. I near No. II was very faint and was not measured. Streamer No. II is well defined though faint. It is sharpest on the concave side. Streamer No. III is a thin streamer well defined at the base and indeed to the point where the streamer reverses its direction of curvature; the top is less definite. Streamers No. V and No. VI are both very definite and are sharp on the convex side.

1908

This eclipse lasted 3 minutes, 52 seconds. Six plates were exposed. I measured plate No. 5, exposed for 64 seconds. Streamer No. I is fairly well defined. Streamer No. IV is of a short bushy type resembling the Bredichin type of comets' tails that are composed of the heavier metals. Streamers No. II, No. III, No. V, and No. VI are clearly defined. All are sharp on the convex side. Streamers No. II and No. III are on the southern extremity of a region that covers an arc of the edge of the shadow about 50° in length. Streamers No. IV, No. V, and No. VI are on the northern extremity of this region. This entire region is covered with complex, ill-defined coronal masses, while the streamers that bound it are clearly defined. Both groups of streamers curve first away from this region, then toward it, so that if the tops of the streamers were produced in the general direction that they are taking there, the two groups would cross each other.

In almost every instance the streamers are sharper on the convex side than on the concave side; that is, if the streamer curves first away from the pole and then toward it, the streamer is sharpest on the side away from the pole. There were two exceptions—noted above—to this statement. In many instances, the larger, well defined streamers were less dense along a line defining the middle of the streamer than on the edges parallel to this line.

TABLE II

Streamer	θ	ϕ	θ_0	ϕ_0	θ'	ϕ'	$\theta-\theta_0$	R	R'	a	e	F*	v_2†
I 1893...	243° 26′	− 9° 51′ 20″	174° 41′	−25° 36′ 35″	286° 50′	−18° 15′ 40″	68° 45′	1.6702	1.0617	5.488	0.822	0.9970	1.6
II 1893...	.....	.....	.....	will not solve	.....	.....	.....	.....	.....	.....	.....	.....	.....
I 1898...	35 45	− 7 16 20	6 54	− 8 6 10	86 34	− 8 6 10	28 51	2.5509	1.0026	3.133	.915	.9937	1.89
II 1898...	99 21	17 54 10	78 2	19 8 10	117 10	19 8 10	21 25	1.9983	1.1504	2.612	.914	.9931	2.09
I 1900...	45 00	−17 42 50	10 00	−21 18 50	60 27	−20 00	35 00	1.4794	1.1066	2.353	.700	.9962	0.64
II 1900...	50 12	−22 21 40	8 2	−29 1 50	71 14	−24 4 10	42 10	1.3893	1.0484	2.431	.645	.9967	0.37
I 1901...	296 34	− 8 38 20	171 55	14 57	327 29	1 30	124 39	2.0000	1.8504	1.850	.459	.9964	very small
II 1905...	248 12	73 16 30	199 50	78 42 40	271 43	76 32 30	48 22	1.2731	1.0084	2.1978	.820	.9988	0.31
III 1905...	251 35	−83 38	191 44	−86 47 20	320 49	−86 47	59 50	1.2760	1.0453	1.5544	.930	.9994	0.16
V 1905...	92 52	−20 47	60 11	−24 17	121 37	−24 17	32 41	1.7649	1.2041	3.262	.84	.9958	0.97
VI 1905...	109 10	−31 25 28	82 40	−34 19	126 11	−34 19	26 30	1.6425	1.2307	2.1870	.829	.9955	1.41
I 1908...	243 26	−71 00	223 11	−72 5 50	254 54	−71 31 50	20 15	1.4107	1.0034	2.043	.958	.9966	1.06
II 1908...	.....	.....	.....	will not solve	.....	.....	.....	.....	.....	.....	.....	.....	.....
III 1908...	.....	.....	.....	will not solve	.....	.....	.....	.....	.....	.....	.....	.....	.....
IV 1908...	248 12	−16 19 50	199 56	−23 45 25	278 44	−21 10 20	48 16	1.6144	1.1006	2.402	.665	.9964	0.48
VI 1908...	251 34	− 7 37 20	208 27	−10 23 20	278 36	−10 23 20	43 07	1.4888	1.0837	4.444	.800	.9966	0.20

* F is the repulsive force acting on these particles. It is measured in terms of the attractive force of the sun.

† v_2 is expressed in miles per second.

This was more noticeable near the sun than at some distance from it. The phenomenon might be accounted for if the streams were hollow. A glance at Table I shows that there were several pairs of streamers.

The two groups of streamers mentioned in connection with the discussion of the streamers of 1908 led me to examine the plates with the view of determining if the type of streamers that I was investigating occurred only, or chiefly, near the disturbed regions of the corona, and therefore were probably the result of local disturbances. There are no streamers of this type in the neighborhood of the disturbed region in the southeast quadrant of the corona of 1908. Neither are there streamers of this type near the disturbed region in the corona of 1905. In the corona of 1901, there is a disturbed region. The one streamer of this year that I measured is about 12° from one edge of this region; on the other side of this region there is no evidence that the coronal streams are affected. It seems to me that the only instances in which we can even suspect that the shape of the stream is due to local disturbances are in the cases of 1900 and 1908. In the former case the streamer lies between the projection of two prominences. There is no way of knowing, however, whether the prominences are on the same side or opposite sides of the sun, and it is equally uncertain regarding the streamers of 1908.

The methods developed in the earlier part of this paper were applied to the sixteen streamers with the results shown in Table II.

The results are much as we should expect. Of the thirteen streamers that gave real solutions, ten originated in the sun-spot zones, three did not. Eight originated below the equator, five above. If this mechanical theory be true, we should, in general, expect that the farther from the equator of the sun the streamer originated, the larger would be the eccentricity of the orbits of the particles composing the stream. Computations bear this out. The average of the eccentricities of the orbits of the particles in the thirteen streams is 0.794, the average of the eccentricities of the orbits of the particles in the three streams nearest the poles is 0.903. The average of the aphelion distance of the particles is 5.1 radii of the sun.

There are three streamers that do not lend themselves to this treatment. One of these, streamer No. II, 1893, is very indefinite; the other two are well-defined streamers apparently meeting all the conditions. They are apparently near each other and resemble each other strikingly. It is possible that their shape may have been influenced by local causes. If this is not so, it would show that at least not all the streamers are caused in the way that we have assumed. However, I believe that the non-agreement of some streamers with theory is what we might naturally expect. The surprise is that so large a percentage of them conformed to the theory.

If this mechanical theory is true, we should expect some streamers to cross the equator. For example, when the eclipse of 1893 occurred, the north pole of the sun was inclined away from us. Hence, if the projections of any stream crossed the projection of the east end of the sun's equator, we should expect them to cross from north to south. That is, the part of the streamer nearest the sun would project into a point north of the equator and those farthest from the sun south of it. With this in view, I examined the plates of each eclipse (except 1905) with the following results:

1893. None crossed east side. On the west side, four crossed the equator from south to north; that is, the base of the streamer is south of the west end of the sun's equator and the top is north of it, as they should be. They are all well defined.

1898. None on the east side. Two streamers on the west side cross from south to north as they should.

1900. No streamers cross the equator.

1901. On the east side, one well defined streamer crosses the equator as it should. On the west side, there are possibly two ill-defined ones. They cross as they should *not*.

1908. Two on the east side cross as they should, none on the west. That is, nine well defined streamers cross the equator, qualitatively at least, as a mechanical theory of the corona would require, and two doubtful ones cross it in the opposite direction.

THE CONVERSE PROBLEM

As a further verification of this theory I attempted two other problems, or rather, two other phases of this problem. The first

may be stated thus: Having assumed for a, e, $\phi_\circ$, and $\theta_\circ$, the set of values obtained for one of the streamers in the foregoing computation, I computed the rectangular co-ordinates of a series of points, which, according to the theory, should be points of the streamer. If one drew a curve through these points, it should be an exact reproduction of the streamer measured on the photographs. The method I adopted is as follows:

Let T = time of the perihelion passage of a particle;
E = eccentric anomaly of the particle at time t.

Then, using the previous notation,

$$n = \frac{\omega \cos \phi_\circ}{a^2 \sqrt{1-e^2}} \tag{15}$$

$$n(t-T) = E - e \sin E \tag{16}$$

$$\tan \frac{w}{2} = \sqrt{\frac{1+e}{1-e}} \tan \frac{E}{2} \tag{17}$$

For a given value of $t-T$ we obtain E from (16); w from (17); $w_\circ$ from (10); ϕ and $\theta_\circ$ from (1) and (3) respectively. By assigning a series of values to $t-T$ we obtain a series of values for each of the other quantities; $\theta_\circ$ is given for one point, and hence a certain value of $\theta - \theta_\circ$ by the previous computation. The $\theta_\circ$ for any other point may be obtained by multiplying ω by the interval that has elapsed from the time one of the particles left the sun until the other did and adding or subtracting the product to the given $\theta_\circ$. We may now obtain a series of values for θ and hence for ξ and η.

I applied the above theory to several of the streamers the orbits of the particles of which we had computed; I found in every instance when the streamer was plotted that the reversal of curvature was exactly as I had measured it on the plate. That is, A, A', and ρ measured as they were on the original photograph had been reproduced in the drawing. There was one feature of the streamers I could not reproduce in this way. The shorter streamers, those that did not go beyond the inner corona, could be reproduced in every detail; but the very long ones would turn back before they reached the distance from the sun shown in the photograph. On Fig. 6 (see p. 327) I have plotted three streamers that are reproduced from the computed value. They are

Streamer No. 20 on Fig. 6 which is Streamer No. III, 1905.
" " 21 " " 6 " " " " II, 1898.
" " 23 " " 6 " " " " V, 1905.

Streamer No. III 1905 is plotted longer than it appeared on the photograph, but the other two are about three-tenths of a sun's radius shorter than they were on the photograph. Moreover it is impossible with the computed values of a, e, and ϕ_0 to produce a streamer that, when plotted, will not turn back toward the sun somewhere near the extremity of the streamer in the drawing. One may find a stream as long as he chooses, but this long stream will not always project into a long streamer.

This discrepancy may be due to one of many causes. It may be due to errors of measurement. For example, in the case of streamer No. V 1905, if the measures of A and A' had been such that $A-A'$ had been decreased by half a degree, the streamer would have reproduced in every detail. Or, if for a given A, ρ had been measured longer, the computed streamer would have been as long as the one on the photograph. Now A', and ρ also, are usually difficult to measure accurately; but it is hardly probable that one would have made a mistake in the wrong direction in the measurement of every long streamer. Or, this discrepancy may be due to the fact that the radiant pressure near the sun's surface does not vary inversely as the square of the distance from the sun's center. Or it may be due to the fact that the particles in the part of the stream farthest from the sun were ejected with a greater force than those near the base of the streamer; or it may be that the particles in the stream are moving in a resisting medium and that this is denser in the inner than in the outer corona. And it may be (and I think this the most likely) that the particles in the end of the stream are finer than those at its base and hence the radiant pressure on them is greater.

But if it be any of these causes, the method of finding the heliocentric position of these streamers is valid. It becomes necessary only to replace equation (8) by the equation of the true orbit. Moreover the fact that all the theoretical results agree so perfectly with the measured values, with the exception noted, shows that the orbits are not very different from an ellipse. It is also worthy

of remark that if a stream of particles, after being ejected from the sun's surface, is acted upon by the attractive force of the sun only, these particles cannot arrange themselves in streams of the shape we have measured.

The statement is susceptible of mathematical proof.

Let the equations of motion of the particles be

$$\frac{d^2x}{dt^2} = -C^2\frac{x}{R^3},$$

$$\frac{d^2y}{dt^2} = -\frac{C^2y}{R^3},$$

$$\frac{d^2z}{dt^2} = -\frac{C^2z}{R^3},$$

where the mass of the sun is unity. Having the elements of the orbit we can determine C, which should be, but never is, equal to the Gaussian Constant—in fact, not even equal approximately to that constant. The reason of course is this: In order that the particles may reach the distances from the sun's surface measured on the photographs, the particles must be ejected with velocity so great that the stream for distances such as we have photographed must be straight lines and hence the streamers will be straight lines. This has long been recognized. Ranyard[1] discussed this at some length in his very exhaustive report to the Royal Astronomical Society. He says:

> We have, therefore, evidence that many rays, especially those seen towards the edges of the synclinal groups, are inclined at considerable angles to the normal to the surface of the photograph. It is difficult to conclude how explosions within a gaseous body like the sun can give rise to oblique rays, but the evidence for the existence of such rays in many coronas, besides that visible during the eclipse of 1871, is overpowering. Some of these oblique rays are straight or nearly straight, while others show considerable curvature and others bend over in one direction in their lower parts and are again carried slightly in a contrary direction above. . . . .
>
> The existence of these curving forms and rays showing contrary flexure is a matter of considerable importance as they appear to indicate the existence of an atmosphere with currents carrying the matter of which the structures are composed with different velocities at different altitudes.

[1] *Memoirs Royal Astronomical Society*, **41**, 487, 1879.

The second problem may be stated as follows:

I assumed arbitrary values of a, e, $\phi_\circ$, and $\theta_\circ$ and computed in the same way a series of streamers. Table III shows the values I assumed. I wished to see if, when the streamers were plotted, the *ensemble* would resemble a photographed corona. I did not attempt to represent any given corona, but rather chose such values as would produce various types of streamers: that is, long ones, short ones, those nearly straight, those curved, streamers originating in various latitudes, etc. I was guided somewhat in my choice of values by the results in Table II. To represent the actual corona, a greater number of streamers should have been plotted in low latitudes. Moreover there should have been a greater number of short streamers, which can be obtained by decreasing $\theta_\circ$, or by decreasing e, or by increasing the major axis.

Fig. 5 and Fig. 6 show coronas resulting from plotting streamers computed from the data given in Table III. The circumference of the circle represents the sun. The points, the position of which we computed, are at the intersection of the streamers and the short lines crossing them. I plotted a good many points—more than necessary—that were projected into the sun to show the direction of the streamer at the margin of the sun.

In Fig. 5[1] λ is assumed to be 90°. Since this is not very different from λ at the time of the eclipse of 1900, the general features of this drawing strikingly resemble those of the corona of that year. The streamers in Fig. 6, except streamers Nos. 20, 21, 22, 23, which occur only on Fig. 6, are computed from the same data as those of Fig. 5; except λ in Fig. 6 is assumed equal 82° 49′ 56″. This is the value of λ at the time of the eclipse of 1905. The streamers which are computed from the same values of $a, e, \phi_\circ$, and $\theta_\circ$ bear the same numbers on the two plates. For example, viewed from the sun's center, streamer No. 3 on both plates would appear the same; that is, with reference to the sun, streamer No. 3 on the two plates is identical. Fig. 5 shows this streamer as it would appear *from the earth* when the axis of the sun was perpendicular

[1] In making the computations for these plates, I was most ably assisted by Mr. Thomas R. Taylor, a Junior in Swarthmore College. He assisted in all the computations, and made the drawing for Fig. 5.

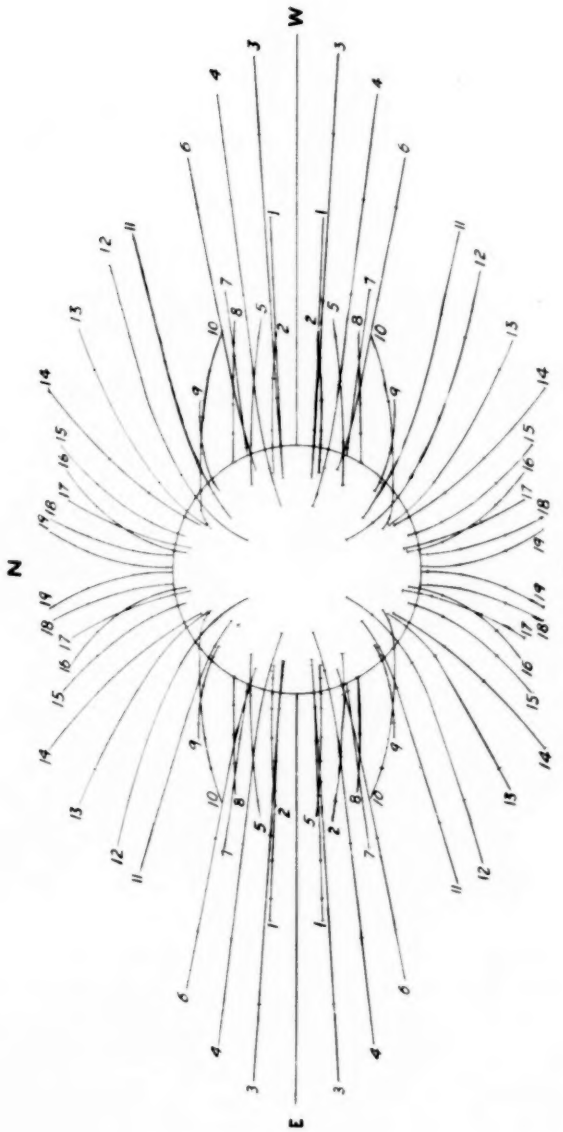

FIG. 5

to the line of sight; and Fig. 6 shows the same streamer as it appears from the earth, when the sun's axis is inclined 82° 49′ 56″ to the line of sight. On Fig. 6 also, streamer No. 22 shows how this same streamer would appear from the earth if the angle between the sun's axis and the line of sight were 95° 21′ 12″ (λ at time of eclipse of 1898). The streamers were numbered as follows. Those in the first quadrant were numbered *seriatim* from the west side of the sun's equator to its north pole. Those in the second quadrant

TABLE III

Streamer	ϕ_0	a	e	θ_0
No. 1.....	5°	3.00	0.915	135° 24′
2.....	10° 23′ 20″	4.44	.800	125 24
3.....	5	6.00	.99	126 4
4.....	10	5.0	.99	109 8
5.....	20	5.0	.82	117 8
6.....	10	5.0	.99	137
7.....	15	3.0	.98	162 02
8.....	25	2.5	.7	105 24
9.....	40	2.5	.7	127 19
10.....	45	5.00	.82	157 52
11.....	25	2.0	.98	155 44
12.....	30	2.0	.98	143 12
13.....	40	2.0	.98	154 06
14.....	55	2.0	.98	140
15.....	65	2.0	.965	140 15
16.....	65	2.0	.965	160 15
17.....	75	2.0	.98	139 20
18.....	80	2.0	.98	139 31
19.....	80	2.0	.98	169 31
20.....	−86 47	1.554	.930	269
21.....	19 8 10	2.612	.914	105 54

were derived from those in the first quadrant by changing θ_0 in the expressions for ξ and η into $180°+\theta_0$. The streamers of the third and fourth quadrants are derived by putting $-\phi$ for ϕ in the expressions for ξ and η in the second and first quadrants respectively. Accordingly the numerical values of ξ and η for corresponding points in the first and third quadrants are equal but their signs are different. The same is true for the corresponding points of the second and fourth quadrants. I have numbered all these streamers thus derived with the same number as the streamer bears from which they were derived. For example, there is a streamer No. 1 in each quadrant of each figure. Streamer No. 1

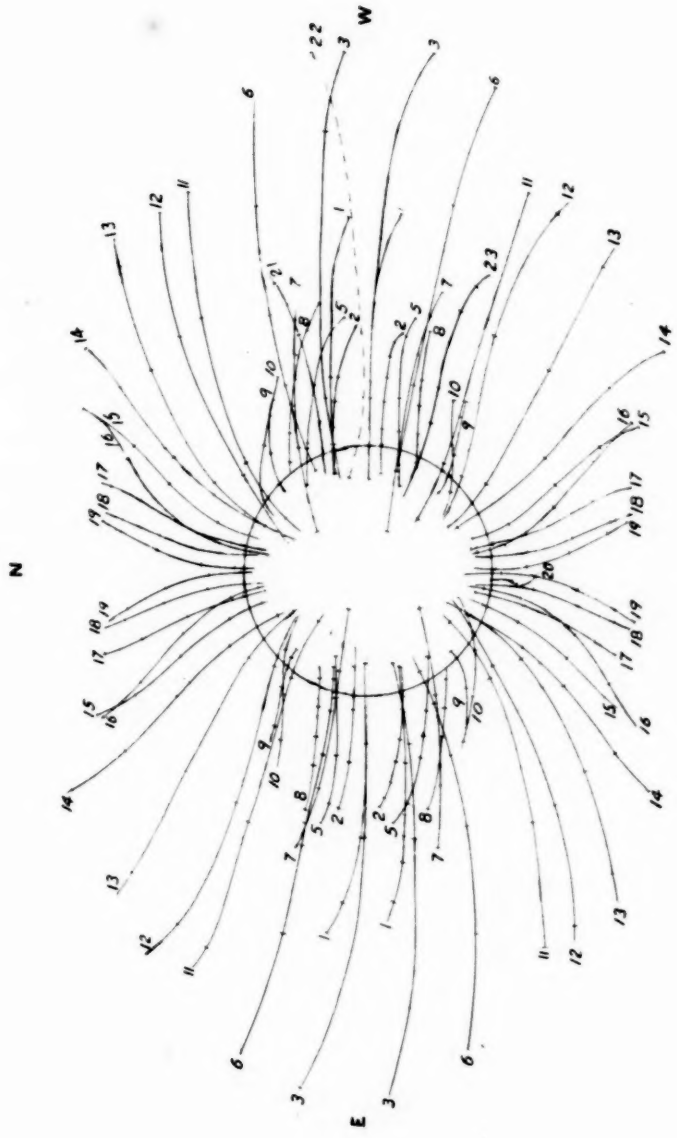

FIG. 6

in the first quadrant is computed from the data given in Table III. Streamer No. 1 in the second quadrant is computed with the same data except θ_0, which has been changed to $180+\theta_0$, and so on. As viewed from the center of the sun they are symmetrical with respect to the sun's equator and also with respect to a meridian of the sun passing through the line of sight.

As we should expect, the streamers in Fig. 5 are symmetrical with respect to the sun's axis, but those of Fig. 6 are not. Streamer No. 13 is typical. There are four points plotted on this streamer. It will be observed that for a given ξ the η of every point in the first quadrant is greater than the η for the corresponding point in the second quadrant and this is in general true for points on the streamers within three radii of the sun from the sun's center. The lack of symmetry with respect to the axis is not as striking as I had anticipated it would be, but would be more striking if the streamers were shorter. I believe the symmetry with respect to a line not coincident with the sun's axis discussed by Ranyard[1] may be accounted for in this way. But if so, the axis of symmetry should be on one side of the axis of the sun when $\lambda > 90^\circ$ and on the other when $\lambda < 90^\circ$.

It has occurred to me since making these computations that we should be able to find on our photographic plates some streamers that turn back toward the sun. By this I do not mean that the streams turn back (though they may do so) but that their projections turn back. If the chief source of the light received from these streamers is reflected sunlight, the long streamers on the west side of the sun should in general be brighter than the long streamers on the east side of the sun. The converse is true of the short streamers. Also one would be more likely to find streamers that turn back on the east side of the sun than on the west side. If the exposures on the photographs of large scale were long enough to photograph longer streamers, a very much greater number could be found that reverse their direction of curvature.

It would seem, from the foregoing results, that it is reasonable to conclude, or at least to assume as a working hypothesis, that the streams of the sun's corona are made of moving particles, obeying

[1] *Op. cit.*, pp. 488 ff.

mechanical laws; that other forces than the attractive force of the sun is acting on these particles; that the shape of the streamers is a function of the inclination of the sun's axis to the line of sight. It is of interest perhaps to note that if a sun-spot is formed from particles ejected above the solar surface, the spot will drift toward the equator unless the particles move in dense resisting media, and that of two such spots at the same height above the solar surface, that will show the shorter period of rotation which originated nearer the equator. The same remarks apply to faculae or any body of particles ejected from the solar surface.

SWARTHMORE COLLEGE
SWARTHMORE, PA.
January 14, 1911

ABOLITION OF TWO OF THE SPHERICAL ERRORS OF A THIN LENS-SYSTEM

By JAMES P. C. SOUTHALL

The essential requirement of an optical image is that it shall be a clear and faithful reproduction of the object to be depicted; but there are numerous and more or less insuperable difficulties in the way of the realization of this aim, which, from the standpoint of geometrical optics, may all be classed under two general heads, viz., aberrations on account of color-dispersion (chromatic aberrations) and aberrations due to sphericity, the so-called spherical aberrations which are encountered in every optical system composed of a series of lenses. So far as the corrections of the color-faults are concerned, the modern optician has an immense advantage over his predecessors on account of the variety of the new kinds of optical glass that are now at his disposal. The favorable circumstance that varieties of glass of equal refractivity but of different dispersion are now available, enables the designer of a system of lenses to postpone the correction of the color-faults until after he has effected the correction of the spherical errors. For our present purposes, therefore, we may leave out of account altogether the color-faults of the image.

The five spherical abberrations of the third order as originally distinguished by Seidel[1] (which are therefore often called the Seidel image-faults) may be enumerated in the following order:[2]

[1] "Zur Dioptrik. Ueber die Entwicklung der Glieder 3-ter Ordnung, welche den Weg eines ausserhalb der Ebene der Axe gelegenen Lichtstrahles durch ein System brechender Medien bestimmen," *Astronomische Nachrichten*, **43**, 289–332, 1856.

[2] For the analytical expressions of the spherical errors of a centered system of spherical refracting surfaces, the reader is referred to the writer's book, *The Principles and Methods of Geometrical Optics, Especially as Applied to the Theory of Optical Instruments* (New York, 1910). The theory of the spherical aberrations is treated in chap. xii. It is worth while to note that the symbols S^{I}, S^{II}, etc., which are used on p. 466 of this book, are not entirely identical with the symbols S_1, S_2, etc., which are employed in this paper. The connections between these two sets of symbols may be exhibited as follows: $S_1 = S^{I}$; $S_2 = S^{II}$; $S_3 = S^{IV} - 3S^{III}$; $S_4 = S^{IV} - S^{III}$; $S'_3 = S^{IV} - 2S^{III}$; $S'_4 = -S^{III}$; $S_5 = S^{V}$.

1. *The Spherical Aberration* proper, or the aberration of the image of the point of the object which lies on the optical axis of the centered system of spherical refracting surfaces. This error will be denoted by S_1.

2. The defect called *Coma*, in consequence of which the definition of parts of the image not on the axis is impaired; which will be denoted by S_2. The equation $S_2=0$ is equivalent also to the famous *Sine-Condition*, which is so important in the optical theories of Helmholtz and Abbe. The so-called Fraunhofer-condition, discovered by Seidel, is included in the sine-condition.

3 and 4. *The Curvatures* of the primary and secondary image-surfaces in consequence of *Astigmatism*. This pair of spherical errors will be denoted by S_3 and S_4. If the two faults S_3, S_4 are both abolished, we obtain a flat, stigmatic image. It may be mentioned, however, that the curvatures of the image depend essentially on the refractivities of the lenses, so that with unsuitable kinds of glass it is impossible by any choice of the geometrical dimensions of the lens-system (radii, thicknesses, distances) to obtain a plane stigmatic image, as was first recognized by Petzval and more clearly still by Seidel.

In order to remedy as far as possible this defect of curvature, designers of optical instruments sometimes compromise on a kind of artificial flattening of the image-field; which consists in contriving so that the so-called "circles of least confusion" of the astigmatic bundles of image-rays shall all be made to fall in a definite transversal image-plane. The curvature of the surface which is the locus of the circles of least confusion is approximately equal to the arithmetical mean of the curvatures of the primary and secondary image-surfaces; accordingly, if the curvature of this surface is denoted by S'_3, we may write:

$$S'_3=\frac{S_3+S_4}{2}.$$

If $S'_3=0$, the image will be more or less plane, but in general not stigmatic.

On the other hand, again supposing that we cannot obtain an image which is both perfectly stigmatic and perfectly plane ($S_3=S_4=0$), we may be content to disregard the curvature-error and to

effect a compromise as to the *Astigmatism;* in which case we can endeavor to make vanish the expression:

$$S'_4=\frac{S_3-S_4}{2}.$$

5. *The Distortion* of the marginal parts of the image, which will be denoted by S_5. Only in case the five conditions

$$S_1=S_2=S_3=S_4=S_5=0$$

are satisfied simultaneously, will the image of a plane object placed at right angles to the optical axis of a centered system of spherical refracting surfaces be at once sharply defined, flat and true, so that it will indeed coincide completely with the so-called Gaussian or theoretical (collinear) image.

Although it is impossible to attain this degree of perfection, we may at least endeavor to design the optical system so as to abolish those faults, which, for the particular type of instrument in view (telescope, microscope, photographic objective, etc.), are the most detrimental to the image, and perhaps also to minimize the residual image-faults. The problem consists therefore in determining the radii, thicknesses, distances, etc., and the kinds of glass in such way that one or more of Seidel's five expressions for the spherical errors will be made to vanish.

On account of the algebraic difficulties involved in the solution of these equations, the method is applicable only to optical systems of comparatively simple structure. The analytical difficulties are very greatly reduced provided we can neglect the thicknesses of the lenses, and a still further simplification will be introduced if we may also disregard the intervals between each pair of successive lenses.

We propose, therefore, to consider here only this simple and more or less fictitious case of an *optical system of infinitely thin lenses all in contact.* If, as is frequently the case, the lenses are to be placed in close juxtaposition, and especially if they are to be cemented together, a preliminary calculation on the assumption that the entire thickness of the system is negligible will be justifiable and will afford the designer at least an accurate basis for further calculation.

We proceed now to give simple and convenient expressions for the conditions of the abolition of *two* of the spherical errors and for the calculation of the residual spherical errors of a system of thin lenses in contact.

If the positions of the optical center and the primary focal point of the i-th lens are designated by A_i and F_i, respectively, the primary focal length of the lens will be equal to F_iA_i. The power of the lens, denoted by ϕ_i, is the reciprocal of the primary focal length. If M_i, M_{i+1} designate the positions of the points where a paraxial ray, emanating originally from the axial object-point M_1, crosses the optical axis, before and after refraction through the i-th lens, and if we put

$$\frac{1}{\mathbf{x}_i} = A_iM_i\,, \quad \frac{1}{\mathbf{x}'_i} = A_iM_{i+1}\,;$$

and, similarly, if $\mathbf{M}_i$, $\mathbf{M}_{i+1}$ designate the positions of the points where a paraxial ray, going originally through the stop-center $\mathbf{M}_1$, crosses the optical axis before and after refraction through the i-th lens, and if we put

$$\frac{1}{\mathbf{x}_i} = A_i\mathbf{M}_i\,, \quad \frac{1}{\mathbf{x}'_i} = A_i\mathbf{M}_{i+1}\,;$$

and, finally, if the refractive index of this lens (supposed to be surrounded by air) and the curvatures of the first and second surfaces are denoted by n_i, c_i, c'_i, respectively; then

$$x'_i - x_i = \mathbf{x}'_i - \mathbf{x}_i = (n_i - 1)(c_i - c'_i) = \phi_i.$$

In the case of a system of m infinitely thin lenses in contact, it is easy to show[1] that Seidel's expression for the spherical aberration along the axis can be put in the form:

$$S_1 = \sum_{i=1}^{i=m} \left\{ \left(\frac{n_i}{n_i - 1}\right)^2 \phi_i^3 + \frac{3n_i + 1}{n_i - 1} x_i\phi_i^2 + \frac{3n_i + 2}{n_i} x_i^2\phi_i - \frac{2n_i + 1}{n_i - 1} c_i\phi_i^2 - \frac{4(n_i + 1)}{n_i} c_ix_i\phi_i + \frac{n_i + 2}{n_i} c_i^2\phi_i \right\}.$$

If, moreover, for the sake of brevity, we put

$$N = \sum_{i=1}^{i=m} \left\{ \frac{n_i}{n_i - 1} \phi_i^2 + \frac{2n_i + 1}{n_i} \phi_ix_i - \frac{n_i + 1}{n_i} \phi_ic_i \right\},$$

[1] See, for example, *The Principles and Methods of Geometrical Optics*, secs. 268, 271.

and if also we remark that for a system of infinitely thin lenses in contact we have:

$$x_i - x_1 = \sum_{r=1}^{r=i-1} \phi_r = \mathbf{x}_i - \mathbf{x}_1 ,$$

and that, consequently we may write:

$$x_i - \mathbf{x}_i = x_1 - \mathbf{x}_1 = a \text{ (say)};$$

it will also not be difficult to show that the general expression of a spherical error of a centered optical system composed of a series of infinitely thin lenses in contact may be expressed as follows:

$$S = pS_1 + a \left\{ qN - a \sum_{i=1}^{i=m} L_i \phi_i \right\} ,$$

where p, q have certain integral values, positive or negative, and L_i denotes a function of n_i. The values of p, q, and L_i corresponding to each of the spherical errors S_1, S_2, etc., are exhibited in the subjoined table:

S	S_1	S_2	S_3	S_4	S'_3	S'_4	S_5
p	+1	+1	−3	−1	−2	−1	−1
q	0	−1	+6	+2	+4	+2	+3
L_i	0	0	$\frac{3n_i+1}{n_i}$	$\frac{n_i+1}{n_i}$	$\frac{2n_i+1}{n_i}$	+1	$\frac{3n_i+1}{n_i}$

Let

$$S = pS_1 + a \left\{ qN - a \sum_{i=1}^{i=m} L_i \phi_i \right\} ,$$

$$S' = p'S_1 + a \left\{ q'N - a \sum_{i=1}^{i=m} L'_i \phi_i \right\} ,$$

$$S'' = p''S_1 + a \left\{ q''N - a \sum_{i=1}^{i=m} L''_i \phi_i \right\}$$

be the expressions of three of the spherical errors of the lens-system. If the first error (S) has been corrected ($S=0$), the condition of the simultaneous abolition of the second error (S'), that is, the condition of the fulfilment of the additional requirement $S'=0$, will be given by the following convenient equation:

$$\sum_{i=1}^{i=m}\left\{ l\frac{n_i}{n_i-1}\phi_i^2+\left(l\frac{2n_i+1}{n_i}+M_i\right)\phi_i x_i-M_i\phi_i\mathfrak{x}_i-l\frac{n_i+1}{n_i}\phi_i c_i\right\}=0$$

where

$$l=p'q-pq',$$
$$M_i=pL'_i-p'L_i.$$

If two spherical errors have been abolished ($S=S'=0$), the magnitude of a third residual spherical error (S'') will depend only on the strengths of the lenses and their refractivities, and will, therefore, not be affected by any further bending of the lenses or by any alteration in the order of sequence of the lenses. Under these circumstances we find in fact:

$$S''=a^2\sum_{i=1}^{i=m}K_i\phi_i,$$

where

$$K_i=\frac{(p''q'-p'q'')L_i+(pq''-p''q)L'_i-(pq'-p'q)L''_i}{pq'-p'q}.$$

The subjoined table exhibits the values of l and M_i for the simultaneous abolition of any pair of the spherical errors denoted by S, S' and also the expressions for K_i corresponding to each one of the residual spherical errors S''. For convenience of printing, the subscript i has been omitted from the letter n in this table. The numerals 1, 2, 3, 4, 3′, 4′, 5 refer to the spherical errors denoted by S_1, S_2, S_3, S_4, S'_3, S'_4, S_5, respectively. It will be observed that in each horizontal row in the table there are always two values $K_i=0$; the first or left-hand one of these corresponds to $S=0$ and the right-hand one to $S'=0$.

As an illustration of the method of procedure, let us suppose that we propose to design an ordinary telescope-objective composed of two thin lenses cemented together, so that $c'_1=c_2$. Since there are three radii to be determined, we can impose three other conditions, which would probably be:

1. A prescribed focal length ($f=1/\phi$);

2. Abolition of the spherical aberration in the center of the field of view ($S_1=0$);

3. Abolition of *coma* ($S_2=0$), whereby not only the center but the adjacent surrounding parts of the field of view will be portrayed distinctly.

l	M_l	K_i						
		1	2	3	4	3′	4′	5
+1	0	0	0	$-\frac{3n+1}{n}$	$-\frac{n+1}{n}$	$-\frac{2n+1}{n}$	−1	$-\frac{3n+1}{n}$
−6	$\frac{3n+1}{n}$	0	$-\frac{3n+1}{6n}$	0	$-\frac{2}{3n}$	$-\frac{1}{3n}$	$\frac{1}{3n}$	$-\frac{3n+1}{2n}$
−2	$\frac{n+1}{n}$	0	$-\frac{n+1}{2n}$	$\frac{2}{n}$	0	$\frac{n+1}{n}$	$\frac{1}{n}$	$-\frac{3n-1}{n}$
−4	$\frac{2n+1}{n}$	0	$-\frac{2n+1}{4n}$	$\frac{1}{2n}$	$-\frac{1}{2n}$	0	$\frac{1}{2n}$	$-\frac{6n+1}{4n}$
−2	+1	0	$-\frac{1}{2}$	$-\frac{1}{n}$	$-\frac{1}{n}$	$-\frac{1}{n}$	0	$-\frac{3n+2}{2n}$
−3	$\frac{3n+1}{n}$	0	$-\frac{3n+1}{3n}$	$\frac{3n+1}{n}$	$\frac{3n-1}{3n}$	$\frac{6n+1}{3n}$	$\frac{3n+2}{3n}$	0
−3	$\frac{3n+1}{n}$	$\frac{3n+1}{3n}$	0	0	$-\frac{2}{3n}$	$-\frac{1}{3n}$	$\frac{1}{3n}$	$-\frac{3n+1}{3n}$
−1	$\frac{n+1}{n}$	$\frac{n+1}{n}$	0	$\frac{2}{n}$	0	$\frac{1}{n}$	$\frac{1}{n}$	$-\frac{n-1}{n}$
−2	$\frac{2n+1}{n}$	$\frac{2n+1}{n}$	0	$\frac{1}{2n}$	$-\frac{1}{2n}$	0	$\frac{1}{2n}$	−1
−1	+1	+1	0	$-\frac{1}{n}$	$-\frac{1}{n}$	$-\frac{1}{n}$	0	$-\frac{n+1}{n}$
−2	$\frac{3n+1}{n}$	$\frac{3n+1}{2n}$	0	$\frac{3n+1}{2n}$	$\frac{n-1}{2n}$	+1	$\frac{n+1}{2n}$	0
+3	$-\frac{6n+2}{n}$	$\frac{3n+1}{n}$	$\frac{3n+1}{3n}$	0	$-\frac{2}{3n}$	$-\frac{1}{3n}$	$\frac{1}{3n}$	0
+1	−2	$\frac{3n-1}{n}$	$\frac{n-1}{n}$	$\frac{2}{n}$	0	$\frac{1}{n}$	$\frac{1}{n}$	0
+2	$-\frac{4n+1}{n}$	$\frac{6n+1}{2n}$	+1	$\frac{1}{2n}$	$-\frac{1}{2n}$	0	$\frac{1}{2n}$	0
+1	$-\frac{2n+1}{n}$	$\frac{3n+2}{n}$	$\frac{n+1}{n}$	$-\frac{1}{n}$	$-\frac{1}{n}$	$-\frac{1}{n}$	0	0

Accordingly, we have the following equations of condition:

$$\phi_1+\phi_2=\phi$$

$$\sum_{i=1}^{i=2}\left\{\left(\frac{n_i}{n_i-1}\right)^2\phi_i^3+\frac{3n_i+1}{n_i-1}x_i\phi_i^2+\frac{3n_i+2}{n_i}x_i^2\phi_i-\frac{2n_i+1}{n_i-1}c_i\phi_i^2 - \frac{4(n_i+1)}{n_i}c_ix_i\phi_i+\frac{n_i+2}{n_i}c_i^2\phi_i\right\}=0,$$

$$\sum_{i=1}^{i=2}\left\{\frac{n_i}{n_i-1}\phi_i^2+\frac{2n_i+1}{n_i}\phi_ix_i-\frac{n_i+1}{n_i}\phi_ic_i\right\}=0.$$

According to the very practical method of calculation given by E. von Höegh,[1] it is best to regard ϕ_1 as the unknown to be first determined: whence we can obtain, without difficulty, the required curvatures of the lens-surfaces. Thus, substituting $x_1+\phi_1$ in place of x_2, and eliminating both ϕ_2 and c_2, we shall obtain finally an equation of the fifth degree in ϕ_1, three of the roots of which will be found to be real; so that there will always be three possible combinations of a pair of cemented lenses of given refractivities, arranged in a given order of sequence, to produce the desired result. The residual aberrations will be given by the following formulae:

$$S_3 = S_5 = -a^2 \sum_{i=1}^{i=2} \frac{3n_i+1}{n_i}\phi_i ;$$

$$S_4 = -a^2 \sum_{i=1}^{i=2} \frac{n_i+1}{n_i}\phi_i ;$$

$$S'_3 = -a^2 \sum_{i=1}^{i=2} \frac{2n_i+1}{n_i}\phi_i ;$$

$$S'_4 = -a^2 \sum_{i=1}^{i=2} \phi_i .$$

Department of Physics
Alabama Polytechnic Institute
Auburn, Ala.
February 1911

[1] "Zur Theorie der zweitheiligen verkitteten Fernrohrobjective," *Zeitschrift für Instrumentenkunde*, **19**, 37–39, 1899.

ON THE EFFECT OF THE GROOVE FORM ON THE DISTRIBUTION OF LIGHT BY A GRATING

By J. A. ANDERSON and C. M. SPARROW

The following paper will aim to give a simple treatment of the theory of a plane reflecting grating—that is, a reflecting surface consisting of a great number of equidistant, similar, parallel grooves all lying in one plane—for the case in which each groove is bounded by a finite number of plane faces. Following the presentation of the theory will be given a short discussion of previous work on the subject, comparing such work with the results here obtained in order to bring out the points of agreement or difference. Finally the theory will be illustrated by application to a few numerical problems of practical interest. Experimental work will here be touched on only incidentally, it being the intention of the writers to elaborate this side of the question in a subsequent paper.

GENERAL THEORY

Notation.—We will consider a groove made up of plane portions $AB, BC, \ldots$ (Fig. 1) and will generally call such a plane portion a *face* in what follows. We will reckon all directions clockwise from the normal to the grating. We will call

$c_1, c_2 \ldots$ the widths of the faces $AB, BC, \ldots$
$\gamma_1, \gamma_2 \ldots$ the directions of the normals to these faces,
$\pi+\phi \ldots$ the direction of the incident light,
$\theta \ldots$ the direction of the diffracted light,
$\theta_k \ldots$ the direction of the spectrum of the k-th order, k being positive when $\theta_k-\theta_0$ is positive,
$a \ldots$ the grating interval.

Simple grating.—By a simple grating we mean a plane grating consisting of alternate strips of transparent and opaque, or of reflecting and non-reflecting, material. The theory of such a grating is given in all works on optics. If the disturbance in any direction θ due to a single slit is of amplitude R_θ and phase δ, we may represent it by a vector in a plane, and the resultant effect of the N slits is obtained by summing these elementary disturbances as vectors. We thus arrive at the result that, if N is large, all the

light is concentrated in the immediate neighborhood of directions θ_k such that $a(\sin\phi+\sin\theta_k)=k\lambda$, where k is the order of the spectrum. The maximum amplitude in these directions occurs when all these elementary disturbances are in phase; it is therefore NR, and hence the maximum intensity is proportional to N^2R^2. As the factor N is independent of the nature of the slit, it follows that the treatment will apply to any plane grating; and the problem thus becomes one of finding R_θ, the amplitude of the disturbance due to a single groove.

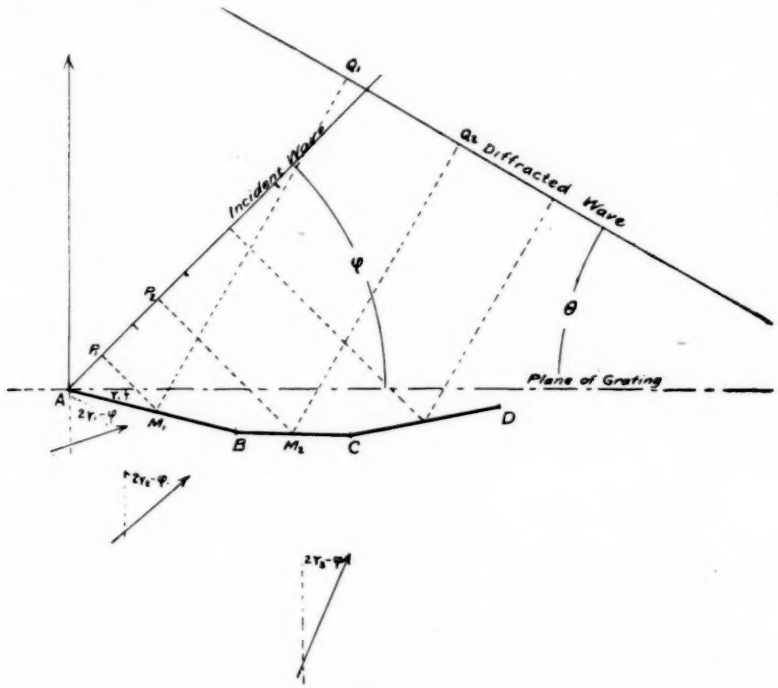

FIG. 1

Only one point needs further mention here. The quantity N^2R^2 is frequently spoken of as being proportional to the "intensity of the spectrum." The term is misleading, and has led to some inaccuracies in the textbooks.[1] The quantity N^2R^2 is the *maximum*

[1] See for example Schuster, *Theory of Optics* (2d ed.), p. 122, where a calculation is made of the efficiency of a grating, neglecting the factor given below.

value of the intensity of illumination in a spectrum line (corresponding to the greatest ordinate in the graph of $y=\sin^2 Nx/\sin^2 x$). But if the resolving power of the grating be sufficient to give us sharp lines, what is actually observed is the *total energy* of the line (corresponding to the area of the above-mentioned curve). To get a number proportional to the total energy we must therefore multiply N^2R^2 by a factor proportional to the width of the line.

Such a factor may be obtained as follows. The difference in path L between the two extreme lines of the grating is

$$L=Na\ (\sin\phi+\sin\theta).$$

If θ is the direction of a principal maximum we obtain the first minimum on either side by making a small change $d\theta$ such that the corresponding change of path is $\pm\lambda$. We thus have

$$dL=\pm\lambda=Na\cos\theta\, d\theta,$$

and the width of the line is $2\lambda/Na\cos\theta$; or for a given wavelength the width varies as $\sec\theta$. We thus get for J the "intensity of the spectrum"

$$J=AR_\theta^2\sec\theta. \tag{1}$$

It remains to calculate R_θ. If we have a single slit in an opaque screen, the usual formula for the amplitude R is

$$R=R_\circ\frac{\sin\alpha}{\alpha}\ ;\ \alpha=\frac{\pi e}{\lambda}(\sin j+\sin\psi), \tag{2}$$

where j is the angle of incidence, ψ the angle of diffraction, e the slit-width, and $R_\circ$ the amplitude in the direction of the incident light. The phase of the disturbance is that at the center of the slit. When $\frac{\pi e}{\lambda}$ is not large, or when we are dealing with directions of diffraction making a considerable angle with the wave normal, the formula is admittedly inadequate, for it takes no account of polarization, and rests on the further assumption that the effect of an element of the wave-front is the same in all directions. The results obtained below will require for their complete accuracy the same limitations; the defect, however, being in no way peculiar to the theory of the composite groove, but belonging equally to the theory of the simple grating as ordinarily given.

General case.—Our method of treating the more general case is a rather obvious extension of the simple theory outlined above. Suppose we have given a groove $ABCD$ . . . . consisting of plane faces AB, BC, CD, ... and that lpane waves are incident on it at an angle ϕ. Each face, such as AB, gives rise to a disturbance whose form we may determine as follows: We construct the direction of regular reflection $2\gamma_1-\phi$ (Fig. 1), and regard AB as a slit in a screen in the plane of AB illuminated by plane waves incident from behind in a direction $2\gamma_1-\phi$. The amplitude P_θ in any direction θ is obtained from (2) by putting $j=\phi-\gamma_1$, $\psi=\theta-\gamma_1$, namely,

$$P=P_\circ\frac{\sin a}{a}\,;\quad a=\frac{\pi c_1}{\lambda}\left[\sin(\phi-\gamma_1)+\sin(\theta-\gamma_1)\right]. \tag{3}$$

The intensity $P_\circ$ at the center of the pattern is proportional to the reflecting power of the surface and to the area of the wave-front falling on AB, so that we may write

$$P=Ar\cos(\phi-\gamma_1)c_1\frac{\sin a}{a} \tag{4}$$

where A depends only on the intensity of illumination, and is therefore the same for all the faces AB, BC, ...

The disturbance due to any other face is given by an expression of the same form as (4). Each of these disturbances will have a definite phase and the resultant effect of the whole groove in the direction θ will be found by adding these separate disturbances as vectors. The phase of any one of these component disturbances may be found by taking the sum of the perpendiculars M_1P_1, M_1Q_1 from the center of the groove face to an arbitrary fixed wave-front and an arbitrary fixed plane normal to the direction θ. The phase is then $\frac{2\pi}{\lambda}$ times this distance, plus the phase-change due to reflection. We thus see that the phase-differences consist of two parts, one depending on the angle of incidence and the other on the angle of diffraction, the two terms being independent of each other. A case of particular interest is offered by the simple triangular groove, with normal illumination on the grating. In this case the difference of path in the direction θ of the disturbances due to the two faces is simply $a/2\cdot\sin\theta$. But the spectra are diffracted in directions θ such that $a\sin\theta=k\lambda$, so that the phase-relation between

the two parts of the groove changes by half a wave-length as we pass from one order to the next; or if β is the phase-difference between the disturbances in the central image, it will be the same in all the even orders, while in the odd orders it will be $\beta+\pi$.

In case the direction of the incident light is such that it does not reach to the bottom of an angle, we must take as our slit the effective portion of the groove-face. If again the direction of reflection is such that the light meets another face of the groove before emerging, we should consider it as reflected from this second face, and take this face as our aperture. Strictly speaking this treatment is only approximate; we should rather regard the second face as illuminated by the first, considering each element of the first face as a source, so that we would have to deal at the second face with light *diffracted* by the first face, not with light regularly reflected. Since, however, the direction of regular reflection coincides with the diffraction maximum, the above method gives an approximate solution. The difficulty should nevertheless be borne clearly in mind, as we shall see that many of the difficulties of numerical computation find their explanation in the complications introduced by multiple reflection.

In the case of metallic reflection the phase-change due to reflection is a function, not only of the angle of incidence, but also of the plane of polarization. The same is true of the reflecting power of the groove-face. As the diffraction formula used here takes no account of polarization, it would be useless labor in applying the theory to take account of these refinements. In the numerical examples given below we have assumed perfect (or at least uniform) reflecting power, and have neglected the phase-change due to reflection. The practical effect of these simplifications can be seen best in a consideration of the detailed results.

To sum up the preceding: The energy of a spectrum which is diffracted in a direction θ is proportional to

$$R^2 \sec \theta,$$

where R is the amplitude of the disturbance due to a single groove. If the groove consist of a number of plane faces, R will be given

by the vector sum of the disturbances due to these faces. If the width c of a face is such that $\frac{\pi c}{\lambda}$ is not small, and if $\phi-\gamma$ is not large, the amplitude of the disturbance due to this face will be given by

$$P=Ar\cos(\phi-\gamma)c\frac{\sin a}{a}\ ;\quad a=\frac{\pi c}{\lambda}[\sin(\phi-\gamma)+\sin(\theta-\gamma)]\ ;$$

and the phase will be a sum of two independent parts, one a function of the angle of incidence, and the other of the angle of diffraction.

PREVIOUS WORK

We have next to consider the relation of the foregoing to previous treatments of the subject. Schuster in his *Theory of Optics* (2d ed., p. 122) considers briefly the question of groove-form in discussing gratings with predominant spectra. He considers a plane face of a groove as giving rise to plane waves of finite extent, and concludes that if these plane waves differ in path by a whole number of wave-lengths they will build up again into a single plane wave, all the light reflected from these faces of the grooves being concentrated into one order. The same point of view is adopted by Trowbridge and Wood[1] in a recent experimental paper, but only as an approximation. Such reasoning ignores the process of diffraction altogether, and is not in our opinion valid. For the only case in which we can consider the groove-face as giving rise to plane waves is when the grating interval is large compared to the wave-length, and in this case the spectra are correspondingly close together, so that the energy is still distributed among several spectra. (The echelon grating furnishes an illustration of this state of things.)

A theory of the effect of groove-form based on the general theory of diffraction is given in a paper by Rowland.[2] The general method used in this paper is sound, but there are errors in the calculation, so that Rowland's final formula is incorrect, as well as

[1] *Phil. Mag.* (6), **20**, 886, 1910.

[2] *Astronomy and Astrophysics*, **12**, 129, 1893; *Phil. Mag.* (5), **35**, 397, 1893; *Rowland's Physical Papers*, p. 525.

a number of his conclusions. When corrected, Rowland's method leads to a formula which, when applied to grooves with plane faces, is equivalent to that obtained above, so far as the value of R is concerned. He likewise neglects, however, the distinction between the intensity of illumination and the energy of the spectrum. As the paper is one which has been rather extensively quoted and referred to, and as the errors seem to have hitherto passed unnoticed, it seems worth while to indicate briefly his general method, showing how his results can be made to agree with ours. The general equations will be simplified to conform to the limitations of the present investigation. Taking a grating in the x z plane, with lines parallel to the z axis, and with illumination perpendicular to these lines, we may ignore the z co-ordinate altogether. If x', y' are the co-ordinates of the source A, x, y the co-ordinates of a point P of the grating surface, and x'', y'' the co-ordinates of a point B of the screen, we may represent the disturbance at x'', y'' due to an element dS of the grating surface by an expression of the form

$$Ae^{-\frac{2\pi i}{\lambda}[\overline{AP}+\overline{PB}]}$$

where A is the amplitude, and the imaginary exponent gives the phase. If we are dealing with parallel light, A will not involve the distance. If χ be the angle between dS and AP, and if we ignore variations in the reflecting power of the surface, we may take A equal to $dS\cos\chi$. In Rowland's paper the factor $\cos\chi$ is overlooked, and A is taken as simply equal to dS—an evident error, for the effect of dS must be proportional to the area of the wave-front which it intercepts. With the notation used above, $\tan\phi=\dfrac{x'-x}{y'-y}$ and $\tan\theta=\dfrac{x''-x}{y''-y}$. Also, if the grating is near the origin as compared with the source and screen, we have approximately

$$\overline{AP}=\sqrt{(x'-x)^2+(y'-y)^2}=\sqrt{x'^2+y'^2}-\frac{xx'+yy'}{\sqrt{x'^2+y'^2}},$$

$$\overline{PB}=\sqrt{(x''-x)^2+(y''-y)^2}=\sqrt{x''^2+y''^2}-\frac{xx''+yy''}{\sqrt{x''^2+y''^2}}.$$

Writing $R=1/\sqrt{x'^2+y'^2}+1/\sqrt{x''^2+y''^2}$,

$$l=\sin\phi+\sin\theta=\frac{x'}{1/\sqrt{x'^2+y'^2}}+\frac{x''}{1/\sqrt{x''^2+y''^2}}\ ,$$

$$m=\cos\phi+\cos\theta=\frac{y'}{1/\sqrt{x'^2+y'^2}}+\frac{y''}{1/\sqrt{x''^2+y''^2}}\ ,$$

we have $\overline{AP}+\overline{PB}=R-(lx+my)$, an equation which becomes exact for parallel light. We have therefore to integrate

$$\int e^{-\frac{2\pi i}{\lambda}[R-lx-my]}\cos\chi\,ds=B\int e^{\frac{2\pi i}{\lambda}(lx+my)}\cos\chi\,dS$$

over the surface of the grating. As the ruling is periodic this breaks up into a number of equal integrals, one over each groove; so that we have only to consider a single groove. If further the groove be made up of a number of plane faces, we may take one of these faces to be

$$x=-y\cot\gamma+b\ ;$$

whence

$$lx+my=(-l\cot\gamma+m)y+lb=$$
$$\frac{-(\sin\phi+\sin\theta)\cos\gamma+(\cos\phi+\cos\theta)\sin\gamma}{\sin\gamma}y+lb=-\frac{\lambda a}{\pi c\sin\gamma}y+b\ ,$$

where $a=\frac{\pi c}{\lambda}[\sin(\phi-\gamma)+\sin(\theta-\gamma)]$ has the same value as in (3),

$$dx=dy\cot\gamma\ ,\quad ds=dy\csc\gamma\ ,\quad \cos\chi=\cos(\phi-\gamma)\ .$$

The integral thus becomes

$$e^{\frac{2\pi ibl}{\lambda}}\cos(\phi-\gamma)\csc\gamma\int_{u_1}^{u_2}e^{-\frac{2ai}{c\sin\gamma}y}\,dy\ ,$$

where u_1 and u_2 are the ordinates of the edges of the face. The integration gives at once

$$\frac{e^{\frac{2\pi ibl}{\lambda}}c\cos(\phi-\gamma)}{-2ia}\left[e^{-\frac{2ia}{c\sin\gamma}u_2}-e^{-\frac{2ia}{c\sin\gamma}u_1}\right].$$

The factor in parentheses can be written

$$-2i\sin\left[\frac{a}{c\sin\gamma}(u_1-u_2)\right]e^{-\frac{a}{c\sin\gamma}(u_1+u_2)}\ ,$$

but $u_1-u_2=c\sin\gamma$, so that we get for the final value of the integral

$$c\cos(\phi-\gamma)\frac{\sin a}{a}e^{i\left[-\frac{a(u_1+u_2)}{c\sin\gamma}+\frac{2\pi bl}{\lambda}\right]}\ . \qquad (5)$$

The real part of this expression gives the amplitude, which is that found above (4). To show that the phase is the same, we take a wave-front through the origin, and a plane through the origin perpendicular to the direction of diffraction. The co-ordinates of the center of the face are

$$\bar{x}=b-\frac{u_1+u_2}{2}\cot\gamma,\quad \bar{y}=\frac{u_1+u_2}{2},$$

and the distances of this point from the planes just mentioned are

$$\left(b-\frac{u_1+u_2}{2}\cot\gamma\right)\sin\phi+\frac{u_1+u_2}{2}\cos\phi,$$

$$\left(b-\frac{u_1+u_2}{2}\cot\gamma\right)\sin\theta+\frac{u_1+u_2}{2}\cos\theta.$$

Adding these two distances we have

$$bl+\frac{u_1+u_2}{2}[-l\cot\gamma+m]=bl-\frac{u_1+u_2}{2}\frac{\lambda}{\pi c}\frac{a}{\sin\gamma},$$

and multiplying by $\frac{2\pi}{\lambda}$ to reduce to angle, we get $\frac{2\pi bl}{\lambda}-\frac{(u_1+u_2)a}{c\sin\gamma}$ as found above (5).

NUMERICAL EXAMPLES

We give below a few examples of how the theory works out in simple cases. As a typical groove we will take a simple triangular groove, consisting of two plane faces which make angles of 15° and −30° respectively with the plane of the grating (Fig. 2 *a*). We will take no account of loss of light by reflection or of phase-change on reflection.

Variation of distribution with wave-length.—In Table I are given the percentages of the total incident energy in the various orders for normal illumination, and for different wave-lengths. The results were obtained by a combination of graphical and numerical methods, the estimated probable error of the computation being about 1 per cent. The wave-lengths are expressed in fractions of the grating interval, the numbers in parentheses below them are the values in $\mu\mu$ which would correspond to a ruling of 10,000 lines to the inch. Three columns are given under each wave-length. The third of these gives the percentage of the total light in the various orders—a quantity which we shall refer to as the

TABLE I

DISTRIBUTION OF ENERGY AS A FUNCTION OF T

Order	0.10 (254)			0.11 (279)			0.12 (305)			0.13 (330)			0.14 (356)			0.15 (381)			0.175	
	AB	*BC*	Total	*AB*	*BC*	Total	*AB*	*BC*	Total	*AB*	*BC*	Total	*AB*	*BC*	Total	*AB*	*BC*	Total	*AB*	*B*
−9.....	0.0	19.7	19.4	0.0	0.2	0.2														
−8.....	0.1	9.9	12.0	0.0	20.7	21.9	0.2	9.8	13.2											
−7.....	0.0	0.1	0.0	0.1	6.3	4.6	0.0	17.8	16.6	0.1	20.7	17.6	0.0	9.3	9.3					
−6.....	0.1	0.6	1.1	0.0	0.0	0.0	0.1	2.2	3.3	0.2	9.6	12.2	0.0	18.0	19.3	0.1	21.8	24.5		
−5.....	0.0	0.1	0.0	0.1	0.5	0.1	0.0	0.2	0.1	0.0	0.2	0.1	0.2	2.5	1.4	0.2	7.7	5.3	0.3	20
−4.....	0.0	0.1	0.3	0.0	0.0	0.1	0.1	0.4	1.0	0.1	0.5	1.2	0.0	0.2	0.3	0.0	0.1	0.1	0.3	5
−3.....	0.1	0.1	0.0	0.1	0.1	0.0	0.0	0.0	0.0	0.1	0.2	0.0	0.2	0.5	0.0	0.2	0.5	0.1	0.0	0
−2.....	0.0	0.0	0.0	0.1	0.1	0.6	0.2	0.1	0.7	0.0	0.1	0.2	0.0	0.0	0.1	0.2	0.2	0.7	0.4	0
−1.....	0.2	0.1	0.0	0.0	0.0	0.0	0.2	0.1	0.0	0.4	0.2	0.0	0.2	0.2	0.0	0.0	0.0	0.0	0.3	0
0.....	0.1	0.0	0.2	0.3	0.1	0.7	0.0	0.0	0.0	0.2	0.0	0.4	0.6	0.1	1.3	0.7	0.2	1.6	0.1	0
1.....	0.0	0.0	0.0	0.5	0.1	0.2	0.7	0.0	0.3	0.1	0.0	0.0	0.1	0.0	0.1	0.9	0.1	0.5	2.2	0
2.....	0.5	0.0	0.8	0.1	0.0	0.1	1.5	0.0	2.2	2.3	0.1	3.2	1.1	0.0	1.6	0.0	0.0	0.0	8.9	0
3.....	2.1	0.1	1.6	2.1	0.0	1.7	0.6	0.0	0.5	9.4	0.1	8.0	25.5	0.1	22.5	41.5	0.1	37.9	52.6	0
4.....	3.7	0.0	4.2	27.0	0.1	29.5	50.0	0.0	52.0	51.7	0.0	52.7	37.6	0.1	40.7	20.3	0.1	23.4	0.3	0
5.....	54.5	0.0	54.0	35.5	0.0	33.1	9.9	0.1	8.4	0.3	0.0	0.2	1.3	0.0	1.0	3.2	0.1	2.3	0.5	0
6.....	3.2	0.0	3.7	1.4	0.0	1.7	3.0	0.1	3.9	0.8	0.1	1.2	0.1	0.0	0.1	1.5	0.0	1.5	65.9	26
7.....	2.0	0.0	1.5	0.0	0.0	0.0	1.6	0.1	1.0	0.6	0.0	0.6	0.8	0.0	0.8	68.8	30.9	07.9		
8.....	1.2	0.1	1.8	0.0	0.0	0.0	1.4	0.0	1.4	66.3	31.8	97.6	67.7	31.0	98.5					
9.....	0.8	0.0	0.8	0.0	0.0	0.0	69.5	30.9	104.6											
	68.6	30.9	101.4	67.3	28.2	94.5														

E I

NCTION OF THE WAVE-LENGTH

)	0.175 (445)			0.20 (508)			0.25 (635)			0.30 (762)			0.40 (1016)			0.50 (1270)		
Total	*AB*	*BC*	Total	*AB*	*BC*	Total	*AB*	*BC*	Total	*AB*	*BC*	Total	*AB*	*BC*	Total	*AB*	*BC*	Total
24.5																		
5.3	0.3	20.7	16.7															
0.1	0.3	5.2	8.0	0.1	14.9	17.7												
0.1	0.0	0.0	0.0	0.1	1.7	1.0	0.3	12.2	8.6	0.1	23.1	19.9						
0.7	0.4	0.5	1.7	0.1	0.1	0.4	0.4	1.2	2.9	0.9	5.8	11.4	0.2	16.5	19.7			
0.0	0.3	0.2	0.0	0.8	0.5	0.0	0.1	0.1	0.0	0.2	0.2	0.0	2.1	3.4	0.4	2.5	7.3	1.3
1.6	0.1	0.0	0.2	0.1	0.1	0.4	2.0	0.5	4.5	1.6	0.3	3.3	0.1	0.1	0.4	4.0	1.0	8.9
0.5	2.2	0.1	1.2	0.6	0.1	0.3	4.1	0.1	2.8	19.3	0.4	13.8	45.5	0.3	38.6	54.5	0.0	54.5
0.0	8.9	0.1	11.1	30.7	0.2	35.5	53.6	0.0	53.6	46.4	0.2	52.8	16.7	0.8	24.6	61.0	8.3	64.7
7.9	52.6	0.0	50.8	33.7	0.2	29.3	2.7	0.1	1.7	2.1	0.0	2.1	64.6	21.1	83.7			
3.4	0.3	0.0	0.4	2.7	0.1	3.9	63.2	14.2	74.1	70.6	30.0	103.3						
2.3	0.5	0.0	0.5	68.9	17.9	88.5												
	65.9	26.8	90.6															
1.5																		
17.9																		

efficiency of the grating. The first and second columns give the percentages which we should have if the faces *BC* and *AB* were blackened successively, all the light being reflected in turn from the 15° and 30° faces respectively. These figures will serve to show in a general way how the phase-relations of the two faces affect the distribution.

A check on the accuracy of the computation is furnished by the condition that the sum of the figures in any column should equal the theoretical total energy. This value is 100 for the columns headed "Total" and 68.3 and 31.7 for the columns headed *AB* and *BC* respectively. The agreement is as good as is to be expected from the rather rough methods employed, as far as $\lambda = 0.15a$. Beyond this value there are irregularities, which we will consider briefly. In the first place the values for *BC* begin to fall short of the theoretical values by considerable amounts. This is due to the fact that the direction of regular reflection from this face of the groove makes such a large angle with the normal to the grating that the center of the diffraction pattern due to this face lies outside the highest order spectrum on that side. The result is that we have light diffracted by this face of the groove in such directions that the energy must be redistributed, by reflection in the other face, among other spectra before it can escape from the grating surface. We are not able to take account of these secondary diffraction phenomena in this elementary treatment, so that this energy is lost to calculation. A second reason for shortage, in the case of the wave-lengths $0.20a$ and $0.25a$, is found in those spectra which escape just at grazing incidence, as this energy must likewise appear in other orders. Finally when the wave-length becomes greater than $0.3a$ the formula (2) becomes quite inaccurate because of the size of the quantity $\frac{\pi c}{\lambda}$.

The effect of the phase-relations of the two faces is greatest, relatively, in the weaker spectra. The phase-relations in a metallic grating would be much more complicated than is assumed here, but the same sort of effect is to be expected in any case, the details of the distribution being of course different.

Another point which is seen immediately is that while the effi-

ciency in the brightest spectrum is a function of the wave-length, it does not increase or decrease continuously with the wave-length, but is periodic. Thus the fifth order for $\lambda = 0.10a$ contains about the same percentage of the total energy as the second order for $\lambda = 0.25a$. The presence of color in the central image is likewise seen to be a property of gratings of this type, it being unnecessary to assume a square groove to explain this phenomenon. It is extremely probable that every form of groove would give such color. The statement made by Rowland (*op. cit.*, p. 6) that in general a simple groove will tend to give a bright first order is not corroborated by this investigation.

FIG. 2

The range of wave-lengths over which a grating will be bright in any one order is a question of some practical interest. Take, for instance, the fourth order in the above table. We find a fairly high efficiency between $0.11a$ and $0.15a$, or between 279 $\mu\mu$ and 381 $\mu\mu$; this spectrum would be very bright in the ultra-violet. With increasing wave-length the range of high efficiency becomes greater; thus the first order is bright from 762 $\mu\mu$ out to the limit of performance of the grating, the exact figures being, however, not obtainable.

Variation of distribution with angle of illumination.—We will now keep a fixed wave-length, and study the effect of varying the angle of incidence. The results of such a calculation are given in Table II, the wave-length chosen being $0.2a$, or green light for a 10,000 ruling.

The figures at the bottom of the table give the theoretical totals for the columns above them. We see that, for all except the first two angles of incidence, the calculated total for the face *BC* falls far short of the theoretical value. The obliqueness of the center of the diffraction pattern is the principal cause of this shortage, to which, however, the small effective width of the face contributes largely. For the angles 30° and 45° the light falling on

TABLE II

DISTRIBUTION OF ENERGY AS A FUNCTION OF THE ANGLE OF INCIDENCE

Order	−30°			−15°			0°			15°			30°			45°			60°		
	AB	*BC*	Total	*AB*	*BC*	Total	*AB*	*BC*	Total	*AB*	*BC*	Total	*AB*	*BC*	Total	*AB*	*BC*	Total	*AB*	*BC*	Total
−7.....	0.0	0.1	0.1																		
−6.....	0.1	10.4	10.5	0.3	4.9	6.6															
−5.....	0.0	17.8	17.8	0.0	18.8	18.0															
−4.....	0.1	9.3	9.4	0.2	9.2	11.3	0.1	14.9	17.7												
−3.....	0.1	1.4	1.5	0.1	0.8	0.5	0.1	1.7	1.0	0.8	7.7	5.1									
−2.....	0.0	0.1	0.1	0.1	0.2	0.4	0.1	0.1	0.4	0.0	0.0	0.1	1.8	8.7	8.5						
−1.....	0.0	0.7	0.7	0.6	0.6	0.4	0.8	0.5	0.0	0.5	0.4	0.2	0.3	3.4	4.1	2.7	1.2	6.9			
0.....	1.2	0.6	1.8	0.4	0.2	0.9	0.1	0.1	0.4	0.8	0.1	1.3	2.3	0.0	2.2	2.9	1.1	0.6	0.5	—	0.5
1.....	3.2	0.3	3.5	0.0	0.0	0.0	0.6	0.1	0.3	0.5	0.0	0.4	0.0	0.2	0.2	5.4	0.9	10.1	32.0	—	32.0
2.....	59.2	0.0	59.2	44.7	0.1	48.1	30.7	0.2	35.5	27.9	0.1	30.5	35.0	0.0	34.7	51.6	0.7	41.9	54.7	—	54.7
3.....	64.9	40.7	105.4	10.5	0.3	8.4	33.7	0.2	29.3	40.2	0.1	37.9	35.9	0.0	36.3	22.3	0.5	26.0	15.9	—	15.9
4.....				56.9	35.2	94.6	2.7	0.1	3.9	0.3	0.0	0.4	0.2	0.0	0.2	1.0	0.3	0.7	2.2	—	2.2
5.....							68.9	17.9	88.5	0.2	0.0	0.1	0.5	0.0	0.5	0.2	0.1	0.6	0.0	—	0.0
6.....										0.2	0.0	0.2	0.8	0.0	0.8	0.7	0.0	0.5	0.3	—	0.3
7.....										71.4	8.4	76.2	0.8	0.0	0.9	0.6	0.0	0.6	0.3	—	0.3
8.....													77.6	12.3	88.4	0.6	0.0	0.3	0.3	—	0.3
9.....																88.0	5.8	88.2	0.4	—	0.4
																			106.6		106.6
	57.7	42.2		63.4	36.6		68.3	31.7		73.2	26.8		78.8	21.2		86.6	12.0		100.0		

BC undergoes a second reflection before escaping from the grating. This sends the center of the pattern off somewhat less obliquely, and the figures show a slight improvement. The second of the causes just mentioned has become more important, however.

Two things strike one at once on examining this table. In the first place, we see that over the entire range of angles considered, the orders 2 and 3 are both bright; so that a casual observer looking at the grating would say that the second and third orders were both bright, regardless of the particular angle at which he might happen to hold the grating. On the other hand, the fluctuations of intensity of these two spectra are by no means less noticeable, so that a measurement of the intensities of the spectra obtained by keeping the bolometer or other energy-measuring device fixed, and rotating the grating, would give results which were in no way comparable with those obtained by keeping the grating fixed and moving the bolometer. Measurements of spectral intensities which involve the former procedure do not therefore give true measurements of the *distribution* of energy.[1]

It seems worth while to consider briefly the effect of certain variations in the groove-form. If we imagine the groove considered above to have its angle determined by the shape of the ruling point, there are two ways by which with a given point we can alter the character of the ruling. In the first place we may alter the depth of the ruling. In the case considered above the entire original surface of the grating plate has been ruled away; if this is not done there will remain flat portions *CD* (Fig. 2 *b*) of the original surface between each groove, and we must now regard the groove as including one of these flat portions. The general effect of this change should be clear in the light of what has been said above. The directions of the diffraction maxima of the oblique faces will be the same as before, but these faces being now smaller, the intensities of the disturbances due to them will be cut down. We shall have, besides, a new disturbance with its maximum in the direction of the central image. The general effect will thus be to

[1] See for instance Wood, *Physical Optics*, p. 179; and Trowbridge and Wood, *op. cit.*, p. 6. The inapplicability of the method is evident when we consider that by rotating the grating we get in all twice as many spectra as the grating can give in any one position.

increase the brightness of the central image at the expense of the other spectra. Phase-relations will no doubt complicate this, but not in such a way as to alter the general character of the effect.

A second way of changing the ruling is by tilting the point in the plane of incidence. The general effect of this should likewise be clear—the direction of maximum efficiency will be shifted to other orders, and in addition the orders on one side will be enhanced at the expense of the others owing to the change in the relative area of the two faces (Fig. 2 *c*).

Practical application.—In conclusion we may inquire how far the results obtained above should be applicable to the case of actual gratings. The limitations of the formula for the diffraction of a single slit are obvious; it takes no account of polarization, and is, moreover, strictly applicable only to the case of wide slits. That it gives reasonably consistent results is itself no criterion for its applicability; an examination of the question from the standpoint of electromagnetic theory could alone answer this question. We have at present, however, no better way of treating diffraction phenomena, save in the case of a single diffracting edge, the complete theory of which has been worked out by Sommerfeld. The phase-changes on reflection assumed above are undoubtedly too simple, but correction on this head seems to offer no insuperable difficulties. The foregoing theory is believed to be at least more complete than any heretofore advanced, though undoubtedly capable of much further improvement. The question may be asked finally, how far the assumption of grooves with plane faces is realized in practice. The pictures of a grating groove given in the textbooks—curved and irregular—may perhaps be taken as indications of current ideas on the subject, so that the triangular groove would appear to many too simple. It is certainly true that no matter how irregular the shape of the grating groove, the grating will be good provided the grooves are identical and equally spaced. The experience of one of the writers, however, who has had charge of the ruling engines in this laboratory during the past year, enables us to state with some assurance the conviction that such gratings have seldom if ever been ruled. In the first place the ruling is done, not with a *point*, as is commonly supposed, but with the

edge of the natural diamond; and it is found that unless the edge is so sharp as to possess no visible width under the highest magnifying power the diamond will not rule; further, that a diamond, after continued use, will cease to rule without the edge showing visible bluntness. The metal of the grating is thus probably not gouged or ploughed out, but pressed aside by the edge, and follows in general the shape of this edge. This view is also borne out by the fact that tilting the diamond in the plane of incidence changes the direction of maximum intensity in the manner to be expected on the above theory. If the groove were simply an irregular scratch this were not to be expected.

PHYSICAL LABORATORY
JOHNS HOPKINS UNIVERSITY
March 3, 1911

PHOTOGRAPHIC DETERMINATIONS OF STELLAR PARALLAX MADE WITH THE YERKES REFRACTOR. V

By FRANK SCHLESINGER

Lalande 25372 ($13^h\,41^m$, $+15°\,26'$)

This is a star of the ninth magnitude having an annual proper motion of 2″.3. The eleven plates secured are described in Table 1.

TABLE 1

PLATES OF *Lalande 25372*

No.	Date	Hour Angle	Observers	Quality of Images	Remarks
200 ...	1904 Jan. 26	$+0^h.2$	S	Poor	
229 ...	Feb. 14	−1.6	S, S	Good	
242 ...	Mar. 3	−0.1	S, Su, S	Fair	
342 ...	May 26	+1.0	S, Su, S	Good	
351 ...	June 4	+1.2	S, F, S	Poor	
581 ...	1905 Jan. 15	−0.4	S, Su, S	Good	
592 ...	Jan. 29	+0.3	S, Su, S	Fair	Second exposure poor
609 ...	Feb. 17	+0.2	S, Su, S	Poor	
618 ...	Feb. 25	−0.1	S, Su, S	Good	
653 ...	Apr. 22	+0.4	F, Su, F	Poor	
683 ...	May 22	+1.2	F, Su, F	Poor	

COMPARISON STARS

No.	DIAMETER	*X* (longitude)	*Y* (latitude)	DEPENDENCE	
				Computed	Adopted
2.....	0.67	+250	−372	−.006	.00
3.....	0.57	+278	0	+.586	+.58
19.....	0.82	−160	+165	+.303	+.30
30.....	0.68	−368	+207	+.117	+.12
Parallax star.	1.03	+ 70.6	+ 75.3		

The parallax star and all the comparison stars except No. 2 are nearly in the same straight line. The dependence on No. 2 under these circumstances is necessarily small; this comparison star was not used in the reductions.

Plates 229, 242, 342, and 351 (two of which have negative parallax factors and two positive) were measured by both Miss Ware and the writer; the others by Miss Ware alone.

TABLE 2

REDUCTIONS FOR *Lalande 25372*

Plate	Solution (m)	Weight (p)	Parallax Factor (P)	Time in Days (t)	Residual (v)	$\sqrt{p}\cdot v$ in Arc
200.....	0.006	0.2	+0.932	−294	+.014	+".02
229.....	0.026	0.8	+0.778	−275	+ 1	.00
242.....	0.046	0.8	+0.554	−257	− 7	−.02
342.....	0.166	1.0	−0.755	−173	0	.00
351.....	0.182	0.5	−0.850	−164	0	.00
581.....	0.801	0.9	+0.973	+ 61	+ 12	+.03
592.....	0.810	0.6	+0.909	+ 75	− 7	−.01
609.....	0.839	0.4	+0.736	+ 94	− 11	−.02
618.....	0.856	0.9	+0.638	+102	− 5	−.01
653.....	0.932	0.4	−0.263	+158	− 4	−.01
683.....	0.989	0.4	−0.705	+188	+ 11	+.02

The normal equations are:

$$\begin{aligned} +3.991\pi - 0.286\mu + 1.973c &= +1.340 \\ +21.776 - 3.717 &= +2.646 \\ +6.900 &= +3.398 \end{aligned}$$

These yield

$$\begin{aligned} c &= +0.597 \\ \mu &= +0.2241 = +0''.596 \\ \pi &= +0.0568 = +\mathbf{0''.152 \pm 0''.007} \end{aligned}$$

Probable error corresponding to unit weight, $\pm 0.0046 = \pm 0''.012$

Other determinations of this parallax are:

Flint (transit circle).....	+0".43	±0".065
Elkin (heliometer).....	+ .17	55
Russell (photography).....	+ .22	19

Fedorenko 2544 ($14^h\ 52^m$, $+54°\ 4'$)

This 8th-magnitude star has an annual proper motion of 1".1. The twelve plates secured were measured in both right ascension

and in declination, and independent values of the parallax derived from the displacements in these two directions.

TABLE 1

PLATES OF *Fedorenko 2544*

No.	Date	Hour Angle	Observers	Quality of Images	Remarks
293 ...	1904 Apr. 26	-2^h0	S, Su, S	Poor	
298 ...	Apr. 28	−0.9	S, Su, S	Poor	
310 ...	May 1	−0.2	S, Su, S	Fair	
320 ...	May 15	−0.4	S, Su, S	Good	
341 ...	May 26	−0.7	S, Su, S	Fair	
350 ...	June 4	−0.4	S, F, S	Poor	
366 ...	June 19	−0.1	Su, S	Poor	
593 ...	1905 Jan. 29	−0.3	S, Su, S	Fair	Star (40) lacking on first exposure
610 ...	Feb. 17	−0.4	S, Su, S	Fair	
619 ...	Feb. 25	−0.8	S, Su, S	Poor	
654 ...	Apr. 22	−0.2	F, Su, F	Fair	
692 ...	June 24	−0.1	F, Su, F	Fair	

COMPARISON STARS

No.	DIAMETER	*X* (right ascension)	*Y* (declination)	DEPENDENCE	
				Computed	Adopted
6.....	1.06	+384	+ 49	+.127	+.125
9.....	0.93	+242	−129	+.042	+.04
21.....	0.71	− 37	− 19	+.162	+.165
24.....	0.77	− 78	−196	+.059	+.06
27.....	0.56	− 98	+258	+.345	+.343
40.....	0.94	−413	+ 37	+.266	+.267
Parallax star.	1.28	− 95	+ 85		

Plates 310, 320, and 366 were measured by both Miss Ware and the writer; the others by Miss Ware alone. Had Miss Ware's measures alone been used for these three plates, none of the quantities m and l would have been changed by more than 0.006 = 0″.016, from those given in Tables 2 and 3.

TABLE 2

REDUCTIONS IN RIGHT ASCENSION FOR *Fedorenko 2544*

Plate	Solution (m)	Weight (p)	Parallax Factor (P)	Time in Days (t)	Residual (v)	$\sqrt{p}\cdot v$ in Arc
293	0.536	0.3	+0.152	−103	+ .014	+″02
298	0.575	0.3	+0.119	−101	+ 56	+ .08
310	0.521	0.8	+0.069	− 98	+ 6	+ .01
320	0.476	1.0	−0.157	− 84	− 21	− .06
341	0.487	0.7	−0.329	− 73	+ 6	+ .01
350	0.449	0.4	−0.463	− 64	− 20	− .03
366	0.444	0.4	−0.660	− 49	+ 6	+ .01
593	0.266	0.7	+0.938	+175	+ 10	+ .02
610	0.230	0.7	+0.919	+194	− 5	− .01
619	0.204	0.4	+0.881	+202	− 23	− .04
654	0.154	0.7	+0.218	+258	− 2	.00
692	0.080	0.7	−0.715	+321	+ 8	+ .02

The normal equations are:

$$+2.284\pi + 2.307\mu + 0.606c = +0.064$$
$$+21.014 \quad +4.245 = -0.338$$
$$+7.100 = +2.518$$

These yield

$$c = +0.414$$
$$\mu = -0.1020 = -0''.271$$
$$\pi = +0.0212 = +0''.056 \pm 0.019$$

Probable error corresponding to unit weight, $\pm 0.0101 = \pm 0''.027$

As will be seen from the next to last column in Table 2, the residual for Plate 298 is unusually large. A solution without this plate yields +0″.050 for the parallax; this is only slightly different from the first value, as we might have anticipated from the low weight and the small parallax factor for this plate. But in this second solution the probable error of the parallax is reduced to 0″.014. Not to overestimate the accuracy of the result, the original solution is regarded as the definitive one.

TABLE 3

REDUCTIONS IN DECLINATION FOR *Fedorenko 2544*

Plate	Solution (m)	Weight (p)	Parallax Factor (P)	Time in Days (t)	Residual (v)	$\frac{1}{15} p \cdot v$ in Arc
293	0.037	0.3	+0.922	−103	−.004	−″01
298	0.050	0.3	+0.930	−101	+ 8	+.01
310	0.068	0.8	+0.941	− 98	+ 24	+.06
320	0.027	1.0	+0.956	− 84	− 24	−.06
341	0.064	0.7	+0.932	− 73	+ 8	+.02
350	0.066	0.4	+0.888	− 64	+ 6	+.01
366	0.056	0.4	+0.770	− 49	− 8	−.01
593	0.167	0.7	−0.186	+175	− 2	.00
610	0.178	0.7	+0.126	+194	− 3	−.01
619	0.200	0.4	+0.254	+202	+ 13	+.02
654	0.213	0.7	+0.902	+258	− 8	−.02
692	0.258	0.7	+0.723	+321	+ 6	+.01

The normal equations are:

$$\begin{aligned} +4.292\pi + 0.439\mu + 4.777c &= +0.463 \\ +21.014 \quad +4.245 &= +1.411 \\ +7.100 &= +0.853 \end{aligned}$$

These yield

$$\begin{aligned} c &= +0.083 \\ \mu &= +0.0501 = +0''.133 \\ \pi &= +0.0105 = +0''.028 \pm 0''.025 \end{aligned}$$

Probable error corresponding to unit weight, $\pm 0.0081 = \pm 0''.022$

Combining the two determinations in accordance with their probable errors we have for the final value

$$\pi = +0''.046 \pm 0''.015$$

Other determinations of this parallax are:

Peter (heliometer)	+0″.08	±0″.022
Flint (transit circle)	− .04	36
Chase (heliometer)	+ .07	40

Weisse I, $17^h 322$ ($17^h 21^m$, $+2^\circ 14'$)

This 8th-magnitude star has a proper motion of 1".4 per annum. Sixteen plates were obtained as described in Table 1; they were measured by Miss Ware alone.

TABLE 1

PLATES OF *Weisse I*, $17^h 322$

No.	Date	Hour Angle	Observers	Quality of Images	Remarks
68...	1903 Aug. 9	$+1^h 7$	S, Su, S	Fair	Telescope East
86...	Sept. 11	+2.2	S, Su, S	Poor	Telescope East
93...	Sept. 20	+2.1	S, S	Fair	Telescope East
259...	1904 Mar. 22	−0.6	S, Su, S	Good	
270...	Mar. 27	−0.7	S, Su, S	Fair	
280...	Apr. 3	−0.4	S, S	Good	
285...	Apr. 17	−0.9	S, Su	Poor	
288...	Apr. 19	−0.4	S, Su, S	Fair	
322...	May 15	+0.6	S, Su, S	Good	
402...	July 28	+1.3	S, Su, S	Fair	
658...	1905 Apr. 22	+0.3	F, Su, F	Poor	
665...	Apr. 28	+0.4	F, Su, F	Fair	
668...	May 6	0.0	F, Su, F	Fair	
694...	June 24	+0.5	F, Su, F	Good	
728...	July 29	+1.8	F, Su, F	Fair	
731...	Aug. 4	+1.4	F, Su, F	Good	

COMPARISON STARS

No.	Diameter	*X* (longitude)	*Y* (latitude)	Dependence	
				Computed	Adopted
13.....	0.70	−231	+201	+.272	+.275
15.....	0.80	− 58	−186	+.451	+.45
18.....	1.10	+ 36	−191	+.379	+.375
22.....	1.20	+253	+176	−.102	−.10
Parallax star.	1.48	−101	−120		

TABLE 2

REDUCTIONS FOR *Weisse I*, 17^h322

Plate	Solution (m)	Weight (p)	Parallax Factor (P)	Time in Days (t)	First Solution Residual (v)	Second Solution Residual (v)
68.....	0.509	0.7	−0.852	−364	+.035	.....
86.....	0.453	0.4	−1.006	−331	+ 4	.....
93.....	0.427	0.5	−0.995	−322	− 18	.....
259.....	0.404	0.9	+0.970	−138	− 24	−.020
270.....	0.444	0.7	+0.948	−133	+ 20	+ 23
280.....	0.402	0.6	+0.906	−126	− 16	− 11
285.....	0.384	0.3	+0.783	−112	− 22	− 16
288.....	0.425	0.7	+0.761	−110	+ 21	+ 27
322.....	0.366	0.9	+0.413	− 84	− 10	+ 1
402.....	0.258	0.7	−0.735	− 10	− 28	− 6
658.....	0.204	0.4	+0.731	+258	+ 1	− 11
665.....	0.201	0.7	+0.658	+264	+ 4	− 7
668.....	0.191	0.7	+0.550	+272	+ 4	− 7
694.....	0.160	0.8	−0.242	+321	+ 32	+ 31
728.....	0.079	0.7	−0.745	+356	− 8	− 5
731.....	0.069	0.9	−0.809	+362	− 12	− 8

The normal equations are:

$$\begin{aligned} +6.253\pi - 0.877\mu + 0.904c &= +0.594 \\ +66.240 + 2.759 &= -2.776 \\ +10.600 &= +3.192 \end{aligned}$$

These yield

$$\begin{aligned} c &= +0.312 \\ \mu &= -0.0543 = -0''.144 \\ \pi &= +0.0424 = +0''.113 \pm 0''.013 \end{aligned}$$

Probable error corresponding to unit weight, $\pm 0.0119 = \pm 0''.032$

We see in Table 1 that the three earliest plates were secured with the telescope east of the pier, while for the others the telescope was (as usual) to the west of the pier. The hour angles for these early plates also differ widely from the others. A second least-

squares solution was therefore undertaken from which these plates were omitted. This yielded

$$c = +0.301$$
$$\mu = -0.0493 = -0''.131$$
$$\pi = +0.0566 = +0''.150 \pm 0''.017$$

Probable error corresponding to unit weight, $\pm 0''.028$

This value of the parallax differs considerably from the former, being $0''.037$ greater. Similar computations in the case of other regions in this list indicate that the reversal of the telescope and the hour-angle error combined have only a slight effect upon the relative position of the parallax star. Nevertheless, as the latter of the two values is entirely free from any such effects, it is probably nearer the truth, in spite of its somewhat greater probable error. As the best value that the present data afford, I therefore adopt

$$+0''.14 \pm 0''.020$$

Other determinations of this parallax are:

Russell (photography)	$+0''.095$	$\pm 0''.012$
Chase (heliometer)	$+ .134$	14
Flint (transit circle, first series)	$+ .17$	55
Flint (transit circle, second series)	$+ .194$	27

The last of these has been kindly communicated by Professor Flint in advance of publication.

Positiones Mediae 2164 ($18^h\,42^m$, $+59^\circ\,29'$)

This well-known double star, otherwise designated as *Struve 2398*, is a system of unusually great interest. The two components are now separated by about $17''$, this distance having increased

nearly 5″ since it was first measured by Struve in 1832. The preceding component is of the 8.7 magnitude and has a spectrum of the K type. The following component emits about half as much visual light: so far as I know its spectrum has never been investigated, but observers report that it is whiter than the other component. The whole system is in rapid motion, 2″.3 per annum.

In 1904[1] I derived a preliminary parallax for this binary from eleven plates taken with the 40-inch telescope. These plates were not competent to determine both the proper motion and the parallax, so that the former was assumed. In this connection it was necessary to allow for the relative motion of the two components. In comparing the position of the fainter component as derived from the plates themselves, with previous micrometric determinations, I noticed that the relative motion must have recently changed its direction by nearly 90°. Measures kindly made at my request by Professor Barnard and Professor Burnham confirmed this, and showed that the pair has comparatively rapid orbital motion, when we consider the great separation and the faintness of the components.

The present determination of the parallax depends upon the twenty-three plates described in Table 1. The distribution in time is excellent, so that the parallax and the proper motions may be determined from them with very small probable errors. This region is close to the pole of the ecliptic, so that the displacements in declination are considerable. The plates were therefore measured in this co-ordinate as well as in right ascension. Furthermore, both components are well measurable and we may therefore derive four nearly independent values of the parallax.

[1] *Astrophysical Journal*, **20**, 129, 1904. This computation is superseded by the present work, in which the same plates are definitively discussed in connection with others secured later.

TABLE 1

PLATES OF *Positiones Mediae 2164*

No.	Date	Hour Angle	Observers	Quality of Images	Remarks
84....	1903 Aug. 20	+1h7	S, Su, S	Good	Telescope East
87....	Sept. 11	+1.6	S, Su, S	Good	Telescope East. Star (28) lacking on first exposure
90....	Sept. 17	+1.8	S. S, S	Good	Telescope East
94....	Sept. 20	+1.4	S, Su, S	Fair	Telescope East
106....	Sept. 27	+0.6	S, Su, S	Good	Telescope East
150....	Nov. 1	+2.1	S, Su, S	Poor	Telescope East
281....	1904 Apr. 3	−1.2	S, Su	Good	
286....	Apr. 17	−1.5	S	Fair	
289....	Apr. 19	−1.2	S, Su, S	Poor	
323....	May 15	−0.3	S, Su, S	Good	
327....	May 17	−0.6	S, Su, S	Good	
335....	May 20	−0.9	S, Su, S	Good	
353....	June 4	−2.0	S, F, S	Good	
427....	Aug. 25	−0.2	S, Su, S	Good	
438....	Aug. 27	−0.4	S, Su, S	Good	Images slightly triangular
443....	Sept. 4	−0.2	S, Su	Poor	Images triangular
659....	1905 Apr. 22	−0.6	F, Su, F	Fair	
664....	Apr. 28	−1.5	F, Su, F	Good	
669....	May 6	−0.9	F, Su, F	Fair	
675....	May 20	−0.5	F, Su, F	Good	
701....	July 15	−0.1	F, Su, F	Good	
749....	Sept. 2	−0.3	Su, Su, Su	Fair	
753....	Sept. 10	0.0	Su, Su, Su	Good	

COMPARISON STARS

No.	DIAMETER	*X* (right ascension)	*Y* (declination)	DEPENDENCE	
				Computed	Adopted
1.....	0.72	−378	+ 62	+.248	+.25
2.....	0.82	− 8	+200	+.480	+.48
3.....	0.72	+ 84	−130	+.115	+.11
4.....	1.58	+302	−132	+.156	+.16
Parallax stars	+1.14	− 41.8	+ 78.4		
	+0.68	− 38.8	+ 72.7		

These dependences were computed with the mean position of the two parallax stars, and apply alike to the reductions for both.

Plates 84 to 106 and 281 to 443 were measured by both Miss Ware and the writer, the other eight by Miss Ware alone.

TABLE 2

REDUCTIONS IN RIGHT ASCENSION FOR THE PRECEDING STAR OF *P.M. 2164*

Plate	Solution (m)	Weight (p)	Parallax Factor (P)	Time in Days (t)	Residual (v)	$\sqrt{p}\cdot v$ in Arc
84.....	1.086	1.0	−0.742	−351	+.005	+″.01
87.....	1.028	1.0	−0.933	−331	− 7	−.02
90.....	1.030	1.0	−0.966	−325	+ 7	+.02
94.....	1.020	0.8	−0.977	−322	+ 2	.00
106.....	1.003	0.8	−0.995	−315	− 4	−.01
150.....	0.964	0.4	−0.869	−280	− 10	−.02
281.....	0.964	0.6	+0.994	−126	− 6	−.01
286.....	0.944	0.4	+0.951	−112	− 2	.00
289.....	0.941	0.5	+0.940	−110	− 2	.00
323.....	0.897	1.0	+0.708	− 84	+ 12	+.03
327.....	0.877	1.0	+0.684	− 82	− 2	−.01
335.....	0.863	1.0	+0.647	− 79	− 8	−.02
353.....	0.829	1.0	+0.436	− 64	− 1	.00
427.....	0.596	0.9	−0.803	+ 18	+ 5	+.01
438.....	0.595	0.8	−0.822	+ 20	+ 8	+.02
443.....	0.564	0.4	−0.891	+ 28	− 5	−.01
659.....	0.461	0.7	+0.923	+258	+ 1	.00
664*.....	0.450	0.9	+0.880	+264	+ 2	+.01
669.....	0.430	0.7	+0.808	+272	+ 1	.00
675.....	0.399	0.9	+0.648	+286	+ 5	+.01
701.....	0.228	0.9	−0.235	+342	0	.00
749.....	0.071	0.7	−0.874	+391	− 26	−.06
753.....	0.093	0.9	−0.931	+399	+ 12	+.03

* Plate 664 was used to illustrate the method of reduction. As a matter of arithmetical convenience, 1.700 has been added to each m.

The normal equations are:

$$+12.117\pi + 11.335\mu - 1.457c = -1.225$$
$$+116.801 - 2.630 = -15.916$$
$$+18.300 = +13.005$$

These yield

$$c = +0.700$$
$$\mu = -0.1307 = -0''.348$$
$$\pi = +0.1055 = +0''.281 \pm 0''.004$$

Probable error corresponding to unit weight, $\pm 0.0051 = \pm 0''.014$

TABLE 3

REDUCTIONS IN RIGHT ASCENSION FOR THE FOLLOWING STAR OF *P.M. 2164*

Plate	Solution (m)	Weight (p)	Parallax Factor (P)	Time in Days (t)	Residual (v)	$\sqrt{p}\cdot v$ in Arc
84.....	1.100	1.0	−0.742	−351	+.004	+″01
87.....	1.060	1.0	−0.933	−331	+ 11	+.03
90.....	1.044	1.0	−0.966	−325	+ 8	+.02
94.....	1.030	0.8	−0.977	−322	− 1	.00
106.....	1.016	0.8	−0.995	−315	− 4	−.01
150.....	0.928	0.4	−0.869	−280	− 57	−.10
281.....	0.980	0.6	+0.994	−126	+ 6	+.01
286.....	0.948	0.4	+0.951	−112	− 2	.00
289.....	0.932	0.5	+0.940	−110	− 16	−.03
323.....	0.884	1.0	+0.708	− 84	− 3	−.01
327.....	0.882	1.0	+0.684	− 82	+ 1	.00
335.....	0.880	1.0	+0.647	− 79	+ 7	+.02
353.....	0.825	1.0	+0.436	− 64	− 6	−.02
427.....	0.593	0.9	−0.803	+ 18	+ 4	+.01
438.....	0.600	0.8	−0.822	+ 20	+ 16	+.04
443.....	0.572	0.4	−0.891	+ 28	+ 6	+.01
659.....	0.455	0.7	+0.923	+258	+ 10	+.02
664.....	0.437	0.9	+0.880	+264	+ 4	+.01
669.....	0.409	0.7	+0.808	+272	− 6	−.01
675.....	0.379	0.9	+0.648	+286	0	.00
701.....	0.203	0.9	−0.235	+342	— 6	−.02
749.....	0.069	0.7	−0.874	+391	− 7	−.02
753.....	0.062	0.9	−0.931	+399	+ 3	+.01

The normal equations are:

$$+12.117\pi + 11.335\mu - 1.457c = -1.282$$
$$+116.801 - 2.630 = -16.476$$
$$+18.300 = +12.985$$

These yield

$$c = +0.698$$
$$\mu = -0.1355 = -0''.360$$
$$\pi = +0.1051 = +0''.280 \pm ''.006$$

Probable error corresponding to unit weight, $\pm 0.0070 = \pm 0''.019$

TABLE 4

REDUCTIONS IN DECLINATION FOR THE PRECEDING STAR OF *P.M. 2164*

Plate	Solution (l)	Weight (p)	Parallax Factor (P)	Time in Days (t)	Residual (v)	$\sqrt{p}\cdot v$ in Arc
84.....	0.008	1.0	+0.672	−351	−.011	−″03
87.....	0.020	1.0	+0.355	−331	− 3	−.01
90.....	0.031	1.0	+0.258	−325	+ 6	+.02
94.....	0.026	0.8	+0.210	−322	+ 1	.00
106.....	0.027	0.8	+0.092	−315	+ 1	.00
150.....	0.036	0.4	−0.482	−280	+ 4	+.01
281.....	0.383	0.6	+0.090	−126	− 12	−.02
286.....	0.456	0.4	+0.323	−112	+ 9	+.02
289.....	0.434	0.5	+0.355	−110	− 20	−.04
323.....	0.546	1.0	+0.722	− 84	+ 1	.00
327.....	0.553	1.0	+0.744	− 82	+ 2	+.01
335.....	0.570	1.0	+0.777	− 79	+ 9	+.02
353.....	0.606	1.0	+0.908	− 64	+ 1	.00
427.....	0.735	0.9	+0.599	+ 18	+ 4	+.01
438.....	0.737	0.8	+0.572	+ 20	+ 5	+.01
443.....	0.754	0.4	+0.454	+ 28	+ 17	+.03
659.....	1.181	0.7	+0.398	+258	+ 3	+.01
664.....	1.192	0.9	+0.489	+264	− 7	−.02
669.....	1.215	0.7	+0.603	+272	− 12	−.03
675.....	1.269	0.9	+0.775	+286	− 4	−.01
749.....	1.443	0.7	+0.487	+391	− 4	−.01
753.....	1.459	0.9	+0.365	+399	+ 10	+.03

The normal equations are:

$$+5.467\pi + 0.480\mu + 8.532c = +6.068$$
$$+106.311 - 5.708 = +17.204$$
$$+17.400 = +10.789$$

These yield

$$c = +0.631$$
$$\mu = +0.1952 = +0''.519$$
$$\pi = +0.1076 = +0''.286 \pm 0''.012$$

Probable error corresponding to unit weight, $\pm 0.0049 = \pm 0''.013$

TABLE 5

REDUCTIONS IN DECLINATION FOR THE FOLLOWING STAR OF *P.M. 2164*

Plate	Solution (l)	Weight (p)	Parallax Factor (P)	Time in Days (t)	Residual (v)	$\sqrt{p}\cdot v$ in Arc
84	0.104	1.0	+0.672	−351	−.010	−″03
87	0.120	1.0	+0.355	−331	+ 7	+.02
90	0.120	1.0	+0.258	−325	+ 6	+.02
94	0.120	0.8	+0.210	−322	+ 7	+.02
106	0.113	0.8	+0.092	−315	0	.00
150	0.087	0.4	−0.482	−280	− 24	−.04
281	0.482	0.6	+0.090	−126	+ 12	+.02
286	0.533	0.4	+0.323	−112	+ 10	+.02
289	0.512	0.5	+0.355	−110	− 19	−.04
323	0.636	1.0	+0.722	− 84	+ 12	+.03
327	0.620	1.0	+0.744	− 82	− 11	−.03
335	0.663	1.0	+0.777	− 79	+ 23	+.06
353	0.673	1.0	+0.908	− 64	− 11	−.03
427	0.784	0.9	+0.599	+ 18	− 18	−.05
438	0.799	0.8	+0.572	+ 20	− 4	−.01
443	0.822	0.4	+0.454	+ 28	+ 18	+.03
659	1.233	0.7	+0.398	+258	+ 1	.00
664	1.253	0.9	+0.489	+264	− 1	.00
669	1.287	0.7	+0.603	+272	+ 4	+.01
675	1.319	0.9	+0.775	+286	− 11	−.03
749	1.486	0.7	+0.487	+391	− 8	−.02
753	1.510	0.9	+0.365	+399	+ 16	+.04

The normal equations are:

$$+5.467\pi + 0.480\mu + 8.532c = +6.685$$
$$+106.311 - 5.708 = +16.161$$
$$+17.400 = +12.067$$

These yield

$$c = +0.697$$
$$\mu = -0.1889 = +0''.503$$
$$\pi = +0.1186 = \mathbf{+0''.314 \pm 0''.019}$$

Probable error corresponding to unit weight, $\pm 0.0077 = \pm 0''.020$

Collecting the results for the parallax we have,

From the right ascensions of the preceding star	+0″.281	±0.004
From the right ascensions of the following star	+ .280	6
From the declinations of the preceding star	+ .286	12
From the declinations of the following star	+ .314	19

The four determinations agree fully as well as we should expect from their probable errors. Combining them in accordance with these errors we have as the definitive parallax of *P.M. 2164*,

$$+0''.282 \pm 0''.003$$

Other determinations are:

Lamp (equatorial micrometer)	$+0''.353$	$\pm 0''.014$
Kostinsky (photography)	$+ .29$	21
Russell (photography)	$+ .296$	31
Flint (transit circle)	$+ .32$	43
Bohlin (photography)	$+ .25$	

These results are unusually accordant and there are few stars whose distances are known with a smaller percentage of probable error than this.

If we examine the residuals for our four solutions in the same way that we did those for *Fedorenko 1457–8* ($9^h\ 8^m$, $+53^\circ\ 7'$) we obtain from the right ascensions

$$\epsilon_1 = \pm 0.0053 = \pm 0''.014$$
$$\epsilon = \pm 0.0000 = \pm 0''.000 \text{ (from Table 2)}$$
$$\epsilon = \pm 0.0046 = \pm 0.012 \text{ (from Table 3)}$$

Here ϵ_1 is the purely accidental error of measurement, and ϵ is a systematic error that tends to shift both parallax stars in the same direction. A similar calculation for the declinations yields,

$$\epsilon_1 = \pm 0.0052 = \pm 0''.014$$
$$\epsilon = \pm 0.0000 = \pm 0.000 \text{ (from Table 4)}$$
$$\epsilon = \pm 0.0058 = \pm 0.015 \text{ (from Table 5)}$$

From these figures we conclude that there may be present a slight tendency to residuals of the same sign for the two parallax stars; but the effect is very small and can be completely accounted for by distortions of the film and the fact that the same comparison stars were used in both cases.

The remarks in Table 1 inform us that the six earliest plates were secured with the telescope east of the pier, whereas all the later ones were secured with the telescope in the usual position, west of the pier. The hour angles for these plates also differ considerably from the others. As the plates secured with the telescope in the usual position cover four parallax maxima, we have

here an excellent opportunity for testing the effect of reversing and the hour-angle error. The first six plates are accordingly omitted and four new least-squares solutions carried out. From the displacements in right ascension of the preceding (brighter) star, I obtain:

$$c = +0.700$$
$$\mu = -0.1308 = -0''.348$$
$$\pi = +0.1050 = +0''.279 \pm 0''.006$$

Probable error corresponding to unit weight, $\pm 0''.015$

From the displacements in right ascension of the following star:

$$c = +0.700$$
$$\mu = -0.1362 = -0''.362$$
$$\pi = +0.1028 = +0''.273 \pm 0''.0045$$

Probable error corresponding to unit weight, $\pm 0''.011$

From the displacements in declination of the preceding star:

$$c = +0.629$$
$$\mu = +0.1949 = +0''.518$$
$$\pi = +0.1136 = +0''.302 \pm 0''.020$$

Probable error corresponding to unit weight, ± 0.014

From the displacements in declination of the following star:

$$c = +0.707$$
$$\mu = +0.1883 = +0''.501$$
$$\pi = +0.1033 = +0''.275 \pm 0''.032$$

Probable error corresponding to unit weight, $\pm 0''.022$

The accordance of these results with those that flow from the use of all the plates is remarkable. The weighted mean value of the parallax is now $+0''.276 \pm 0''.004$, which is $0''.006$ less than before. In right ascension, the new weighted mean is less by just this amount, $0''.006$; while that in declination (which has much lower weight) remains unchanged. An equally good agreement exists between the two sets of proper motions. We therefore conclude that for this region at least, the reversal of the telescope and the hour-angle error have had no appreciable effect upon the relative positions of the parallax stars. We shall return to this subject later in connection with other stars and in a general discussion.

Lamont 18180 ($18^h\,53^m$, $+5°\,48'$)

This 9th-magnitude star has a proper motion of 1".2 per annum. Twenty-one plates were secured, as described in Table 1; these were all measured by Miss Ware.

TABLE 1

PLATES OF *Lamont 18180*

No.	Date	Hour Angle	Observers	Quality of Images	Remarks
19....	1903 June 14	−1h0	S, S, S	Poor	
20....	June 14	+0.2	S, S, S, S	Fair	
57....	Aug. 2	+0.8	S	Poor	Telescope East
76....	Aug. 16	+1.7	S, Su, S	Good	Telescope East. Images elongated on second exposure
107....	Sept. 27	+0.3	S, Su, S	Good	Telescope East
111....	Oct. 11	+2.6	S, Su, S	Good	Telescope East
136....	Oct. 25	+1.7	S, Su, S	Good	Telescope East
324....	1904 May 15	0.0	S, Su, S	Good	
328....	May 17	−0.4	S, Su, S	Good	
336....	May 20	−0.6	S, Su, S	Poor	
346....	May 26	−0.7	S, Su, S	Fair	
428....	Aug. 25	+0.2	S, Su, S	Good	
439....	Aug. 27	0.0	S, Su, S	Good	
455....	Sept. 11	+0.2	S, Su, S	Good	
666....	1905 Apr. 28	−0.7	F, Su, F	Good	
670....	May 6	−0.6	F, Su, F	Good	
676....	May 20	0.0	F, Su, F	Good	
686....	May 30	+0.2	F, Su, F	Good	
732....	Aug. 4	+0.4	F, Su, F	Good	
745....	Aug. 26	0.0	Su	Good	
754....	Sept. 10	+0.7	Su, Su	Fair	

COMPARISON STARS

No.	Diameter	*X* (longitude)	*Y* (latitude)	Dependence	
				Computed	Adopted
1.....	1.65	−162	− 52	−.277	−.25
3.....	0.61	− 45	+ 93	+.329	+.333=⅓
4.....	0.66	+ 6	+ 78	+.403	+.40
5.....	0.80	+ 80	−144	+.023	+.017=1/60
7.....	0.72	+121	+ 25	+.521	+.50
Parallax star.	0.88	+ 97	+ 90		

TABLE 2

REDUCTIONS FOR *Lamont 18180*

Plate	Solution (m)	Weight (p)	Parallax Factor (P)	Time in Days (l)	First Solution Residual (v)	Second Solution Residual (v)
19.....	0.320	0.4	+0.386	−420	+.002	+.011
20.....	0.288	0.8	+0.385	−420	− 30	− 20
57.....	0.318	0.2	−0.422	−371	+ 30	.....
76.....	0.281	0.8	−0.622	−357	+ 1	.....
107.....	0.250	0.9	−0.982	−315	− 10	.....
111.....	0.277	0.9	−0.997	−308	+ 19	.....
136.....	0.269	0.8	−0.954	−287	+ 17	.....
324.....	0.216	0.9	+0.775	− 84	− 7	− 4
328.....	0.227	0.8	+0.753	− 82	+ 6	+ 7
336.....	0.202	0.4	+0.720	− 79	− 18	− 16
346.....	0.238	0.7	+0.644	− 73	+ 22	+ 24
428.....	0.145	0.9	−0.742	+ 18	− 17	− 9
439.....	0.147	0.9	−0.766	+ 20	− 14	− 5
455.....	0.170	0.9	−0.902	+ 35	+ 16	+ 25
666.....	0.107	0.9	+0.925	+264	− 12	− 16
670.....	0.134	0.9	+0.865	+272	+ 19	+ 15
676.....	0.129	0.8	+0.721	+286	+ 21	+ 17
686.....	0.088	0.9	+0.595	+296	− 14	− 18
732.....	0.061	0.9	−0.460	+362	− 1	0
745.....	0.031	0.4	−0.751	+384	− 19	− 17
754.....	0.032	0.5	−0.893	+399	− 10	− 7

The normal equations are:

$$+9.250\pi + 8.820\mu - 1.234c = -0.320$$
$$+113.158 - 1.558 = -3.607$$
$$+15.600 = +2.859$$

These yield

$$c = +0.182$$
$$\mu = -0.0308 = -0''.082$$
$$\pi = +0.0191 = +0''.051 \pm 0''.009$$

Probable error corresponding to unit weight, $\pm 0.0100 = \pm 0''.027$

The five plates from 57 to 136 inclusive were taken with the telescope east of the pier. A second solution was carried out from which these plates were omitted and the following values resulted:

$$c = +0.177$$
$$\mu = -0.0290 = -0''.077$$
$$\pi = +0.0246 = +0''.065 \pm 0''.010$$

Probable error corresponding to unit weight, $\pm 0''.026$

This value of the parallax is 0″.014 greater than the former. We may adopt

$$+0''.06 \pm 0''.012$$

as being the best that can be derived from the present data.

From plates secured at Cambridge (England) Russell has recently obtained $+0''.076 \pm 0''.065$ for this parallax.

Lamont 18816 ($19^h\ 2^m$, $+7°\ 29'$)

This 9th-magnitude star has a proper motion of 0″.8 per annum. The eleven plates secured were all measured by Miss Ware.

TABLE 1

PLATES OF *Lamont 18816*

No.	Date	Hour Angle	Observers	Quality of Images
429	1904 Aug. 25	+0^h.6	S, Su, S	Fair
440	Aug. 27	+0.4	S, Su, S	Fair
456	Sept. 11	+0.6	S, Su, S	Good
667	1905 Apr. 28	−0.5	F, Su	Poor
671	May 6	−0.2	F, Su, F	Poor
733	Aug. 4	+0.8	F, Su, F	Fair
737	Aug. 19	+1.4	F, Su, F	Fair
773	Sept. 17	0.0	Su, Su, Su	Fair
932	1906 May 8	−1.1	Su, J, Su	Poor
933	May 8	−0.7	Su, J, Su	Poor
935	June 5	−0.8	Su, J, Su	Fair

COMPARISON STARS

No.	DIAMETER	*X* (longitude)	*Y* (latitude)	DEPENDENCE	
				Computed	Adopted
7	0.48	+193	− 43	+.137	+.143 = $\frac{1}{7}$
10	0.66	+110	+201	+.274	+.286 = $\frac{2}{7}$
27	1.18	−133	− 66	+.290	+.286 = $\frac{2}{7}$
29	1.36	−170	− 92	+.299	+.286 = $\frac{2}{7}$
Parallax star.	1.33	− 33.3	+ 2.5		

TABLE 2

REDUCTIONS FOR *Lamont 18816*

Plate	Solution (m)	Weight (p)	Parallax Factor (P)	Time in Days (t)	Residual (v)	$\sqrt{p}\cdot v$ in Arc
429	0.364	0.7	−0.709	−282	+.006	+".01
440	0.354	0.7	−0.731	−280	− 3	−.01
456	0.344	0.9	−0.879	−265	− 4	−.01
667	0.263	0.3	+0.943	− 36	− 3	.00
671	0.262	0.4	+0.889	− 28	+ 1	.00
733	0.207	0.7	−0.415	+ 62	+ 6	+.01
737	0.193	0.7	−0.630	+ 77	+ 2	.00
773	0.169	0.7	−0.922	+106	− 4	−.01
932	0.072	0.4	+0.876	+339	− 18	−.03
933	0.102	0.4	+0.875	+339	+ 12	+.02
935	0.073	0.7	+0.557	+367	0	.00

The normal equations are:

$$+3.828\pi + 7.328\mu - 1.447c = -0.632$$
$$+37.538 \quad +0.457 = -1.549$$
$$+6.600 = +1.516$$

These yield

$$c = +0.236$$
$$\mu = -0.0467 = -0''.124$$
$$\pi = +0.0137 = +0''.036 \pm 0''.007$$

Probable error corresponding to unit weight, $\pm 0.0039 = \pm 0''.010$

No other determination of this parallax has been published.

31 b Aquilae ($19^h\ 20^m$, $+11^\circ\ 44'$)

This star has a proper motion of about 1″ a year. It is of the 5th magnitude and accordingly the rotating disk was used to reduce its brightness to the mean for the comparison stars. The ten plates secured were measured by Miss Ware.

TABLE 1

PLATES OF *31 b Aquilae*

No.	Date	Hour Angle	Observers	Quality of Images	Remarks
467....	1904 Sept. 22	+0h2	S, Su, S	Fair	Star (4) partly occulted on first exposure and lacking on second
469....	Sept. 24	+0.5	S, Su, S	Fair	Star (4) lacking on third exposure
493....	Oct. 6	+1.0	S, S, S	Fair	Star (4) lacking on first exposure
695....	1905 June 24	+0.8	F, Su, F	Fair	Star (1) lacking on second exposure
734....	Aug. 4	+1.2	F, Su, F	Good	
738....	Aug. 19	+1.9	F, Su, F	Fair	
774....	Sept. 17	+0.3	Su, Su, Su	Fair	
936....	1906 June 5	−0.4	Su, J, Su	Fair	
937....	June 5	0.0	Su, J, Su	Fair	
938....	June 5	+0.4	Su, J, Su	Good	

COMPARISON STARS

No.	DIAMETER	*X* (longitude)	*Y* (latitude)	DEPENDENCE	
				Computed	Adopted
2.....	0.72	−231	−254	+.135	+.125
3.....	0.63	−156	+ 48	+.200	+.20
4.....	0.92	− 49	− 82	+.181	+.20
6.....	0.53	+312	−134	+.192	+.20
7.....	0.98	+124	+422	+.292	+.275
Parallax star.	0.69	+ 25	+ 58		

TABLE 2

REDUCTIONS FOR *31 b Aquilae*

Plate	Solution (m)	Weight (p)	Parallax Factor (P)	Time in Days (t)	Residual (v)	$\sqrt{p} \cdot v$ in Arc
467	0.019	0.6	−0.916	−254	.000	″00
469	0.018	0.7	−0.929	−252	− 2	.00
493	0.042	0.8	−0.997	−230	+ 7	+.02
695	0.283	0.8	+0.360	+ 21	− 7	−.02
734	0.305	0.9	−0.319	+ 62	+ 8	+.02
738	0.292	0.7	−0.547	+ 77	− 8	−.02
774	0.304	0.7	−0.876	+106	− 8	−.02
936	0.577	0.7	+0.641	+367	− 3	−.01
937	0.561	0.7	+0.640	+367	− 19	−.04
938	0.603	0.9	+0.640	+367	+ 23	+.06

The normal equations are:

$$+3.791\pi + 9.213\mu - 1.520c = +0.497$$
$$+45.109 + 5.320 = +5.379$$
$$+7.500 = +2.315$$

These yield

$$c = +0.259$$
$$\mu = +0.0808 = +0''.215$$
$$\pi = +0.0380 = +\mathbf{0''.101 \pm 0''.022}$$

Probable error corresponding to unit weight, $\pm 0.0080 = \pm 0''.021$

Other determinations of this parallax are:

Peter (heliometer) ..... +0″.06	±0″.010
Flint (transit circle) ..... +0.01	30
Chase (heliometer) ..... +0.02	37

[*To be continued*]